http://dx.doi.org/10.5935/0103-5053.20130144

J. Braz. Chem. Soc., Vol. 24, No. 7, 1099-1108, 2013.
Printed in Brazil - ©2013 Sociedade Brasileira de Química
0103 - 5053 $6.00+0.00

Article

Debromination of *endo*-(+)-3-Bromocamphor with Primary Amines

Svetlana Marković,[a] Violeta Marković,[a] Milan D. Joksović,[a] Nina Todorović,[b] Ljubinka Joksović,*,[a] Vladimir Divjaković[c] and Snežana Trifunović[d]

[a]*Department of Chemistry, Faculty of Science, University of Kragujevac, 12 R. Domanovića, 34000 Kragujevac, Serbia*

[b]*Institute for Chemistry, Technology and Metallurgy, 12 Njegoševa, 11000 Belgrade, Serbia*

[c]*Department of Physics, University of Novi Sad, 3 Trg D.Obradovića, 21000 Novi Sad, Serbia*

[d]*Faculty of Chemistry, University of Belgrade, 16 Trg Studentski, PO Box 158, 11000 Belgrade, Serbia*

A desbromação redutiva da *endo*-(+)-3-bromocânfora com diferentes aminas primárias seguida da formação de imina foi investigada. Esta reação requer procedimento experimental simples sem qualquer solvente orgânico, metal ou agente de redução convencional. Observou-se uma forte influência da polaridade da amina na eficiência do processo de desbromação, e que etanolamina e etilenodiamina tendo pontos de ebulições elevados o suficiente podem desbromar 3-bromocânfora fornecendo canfoniminas em bons rendimentos. Os mecanismos de desbromação da 3-bromocânfora com etanolamina e *n*-hexilamina foram investigados no nível B3LYP/6-311+G(d,p). Revelou-se o mecanismo radical, e que a reação com etanolamina mais polar é energeticamente mais favorável.

Reductive debromination of *endo*-(+)-3-bromocamphor with different primary amines followed by imine formation was investigated. This reaction requires simple experimental procedure without any organic solvent, metal or conventional reducing agent. A strong influence of amine polarity on the efficacy of debromination process was observed, and ethanolamine and ethylene diamine having sufficiently high boiling points can debrominate 3-bromocamphor giving corresponding camphanimines in good isolated yields. The mechanisms of debromination of 3-bromocamphor with ethanolamine and *n*-hexylamine were investigated at the B3LYP/6-311+G(d,p) level of theory. The radical mechanism was revealed, and it was shown that the reaction with more polar ethanolamine is energetically more favorable.

Keywords: 3-bromocamphor, primary amines, reductive debromination, reaction mechanism, DFT

Introduction

The debromination of α-bromoketones plays an important role in the synthetic organic chemistry as one of the most useful reaction for the construction of more complex organic molecules. A number of reagents have been reported for the debromination of α-bromocarbonyl compounds such as triphenylphosphine,[1] pyridinium salts,[2] molybdenum hexacarbonyl,[3] sodium iodide-chlorotrimethylsilane,[4] triphenylphosphonium iodide,[5] sodium borohydride-antimony tribromide,[6] sodium amalgam,[7] tributyltin hydride,[8] zinc in acetic acid,[9] aqueous titanium trichloride,[10] tellurium reagents,[11] nickel boride,[12] selenium,[13] sodium dithionite,[14] inorganic phosphorus compounds[15] and ionic liquids.[16]

On the other hand, a central need of different synthetic transformations in the last years, especially in pharmaceutical industry, is the preparation of compounds that are derived from the chiral sources. Among these compounds, *vic*-amino alcohols obtained from D-camphor[17] and ketimines prepared from camphor-imine[18] serve as template for many applications in asymmetric synthesis. Camphor-based imino alcohols are precursors for preparation of chiral aryl phosphates in the role of

*e-mail: ljubinka@kg.ac.rs

P, *N*-bidentate ligands for asymmetric catalysis by metal complexes.[19]

In conjunction with these facts, herein we report the synthesis of a series of imino compounds containing camphane scaffold derived from *endo*-(+)-3-bromocamphor, accompanied with its simultaneous reductive debromination. In addition, a mechanism for the model reaction, i.e., that of 3-bromocamphor with ethanolamine, is proposed.

Experimental

Materials and methods

All amines were obtained from commercial sources and distilled before use while *endo*-(+)-3-bromocamphor was purchased from Fluka and used without further purification. Melting points were determined on a Mel-Temp capillary melting point apparatus, model 1001 and are uncorrected. IR spectra were recorded on a Perkin Elmer Spectrum One FTIR spectrometer. All ^{1}H and ^{13}C nuclear magnetic resonance (NMR) spectra were recorded on a Bruker Avance III 500 MHz spectrometer. The full assignments of all reported NMR signals were made by use of 1D and 2D NMR experiments.

X-ray crystal structure determination

Single colorless crystal was selected and glued on glass fiber. Diffraction data were collected on an Oxford Diffraction KM4 four-circle goniometer equipped with Sapphire CCD detector. The crystal to detector distance was 45.0 mm and a graphite monochromated Mo K_α ($\lambda = 0.71073$ Å) radiation was employed in the measurement. The frame width of 1° in ω, with experimental time of 2.5 s was used to acquire each frame. More than one hemisphere of three-dimensional data was collected in the measurement. The data were reduced using the Oxford Diffraction program CrysAlis^{Pro}.[20] A semiempirical absorption-correction based upon the intensities of equivalent reflections was applied,[21] and the data were corrected for Lorentz, polarization and background effects. Scattering curves for neutral atoms, together with anomalous-dispersion corrections, were taken from International Tables for X-ray Crystallography.[22] The structure was solved by direct methods,[23] and the figures were drawn using Mercury.[24] Refinements were based on F^2 values and done by full-matrix least-squares[25] with all non-H anisotropic atoms. The positions of all non-H atoms were located by direct methods. The positions of hydrogen atoms were found from the inspection of the difference Fourier maps. The final refinement included atomic positional and displacement parameters for all non-H atoms. At the final stage of the refinement, H atoms were positioned geometrically (O–H = 0.82, N–H = 0.86 and C–H = 0.96-0.98 Å) and refined using a riding model with fixed isotropic displacement parameters. Crystallographic data for the structural analysis were deposited with the Cambridge Crystallographic Data Centre, CCDC No. 824664 for compound $\mathbf{2_A}$.

General procedure for synthesis of debrominated imines $\mathbf{2_{A-F}}$

A mixture of *endo*-(+)-3-bromocamphor (1.156 g, 5 mmol) and corresponding amine (50 mmol) in a 25 mL round-bottomed flask was heated at 130-135 °C in an oil bath for 12 or 24 h. After removal of the excess of the amine under reduced pressure, 30 mL of water were added and the mixture was extracted with ether (40 mL). The organic layer was washed with water (2 × 30 mL). After drying with anhydrous sodium sulfate, the solvent was evaporated and pure compounds were isolated by column chromatography on silica gel using different eluent mixtures.

Computational details

All calculations were conducted using the Gaussian 09 program package, Revision A.02[26] at the B3LYP/6-311+G(d,p) level of theory.[27,28] This triple split valence basis set adds p functions to hydrogen atoms in addition to the d and diffuse functions on heavy atoms. The geometries of all participants in the reactions with ethanolamine (dielectric constant = 30.83)[29] and *n*-hexylamine (dielectric constant = 4.08)[30] were fully optimized by applying the conductor-like polarizable continuum (CPCM) solvation model.[31,32] All radical species were evaluated by using an unrestricted scheme in order to take spin polarization into account. Vibrational analysis was performed for all structures. All calculated structures were confirmed to be energy minima (all real vibrational frequencies) for equilibrium structures, or first-order saddle points (one imaginary vibrational frequency) for transition state structures. To verify that each transition state is linked with two putative minima, the intrinsic reaction coordinates (IRCs), from the transition states down to the two lower energy structures, were traced using the IRC routine in Gaussian. The natural bond orbital (NBO) analysis was performed for all structures using the GenNBO 5.0 program.[33] Relative energies for the reactions with ethanolamine and *n*-hexylamine were calculated at 385 and 405 K (112 and 122 °C), respectively (experimental temperatures).

To estimate homolytic dissociation enthalpies of the C–Br and C–H bonds in some participants the gas-phase

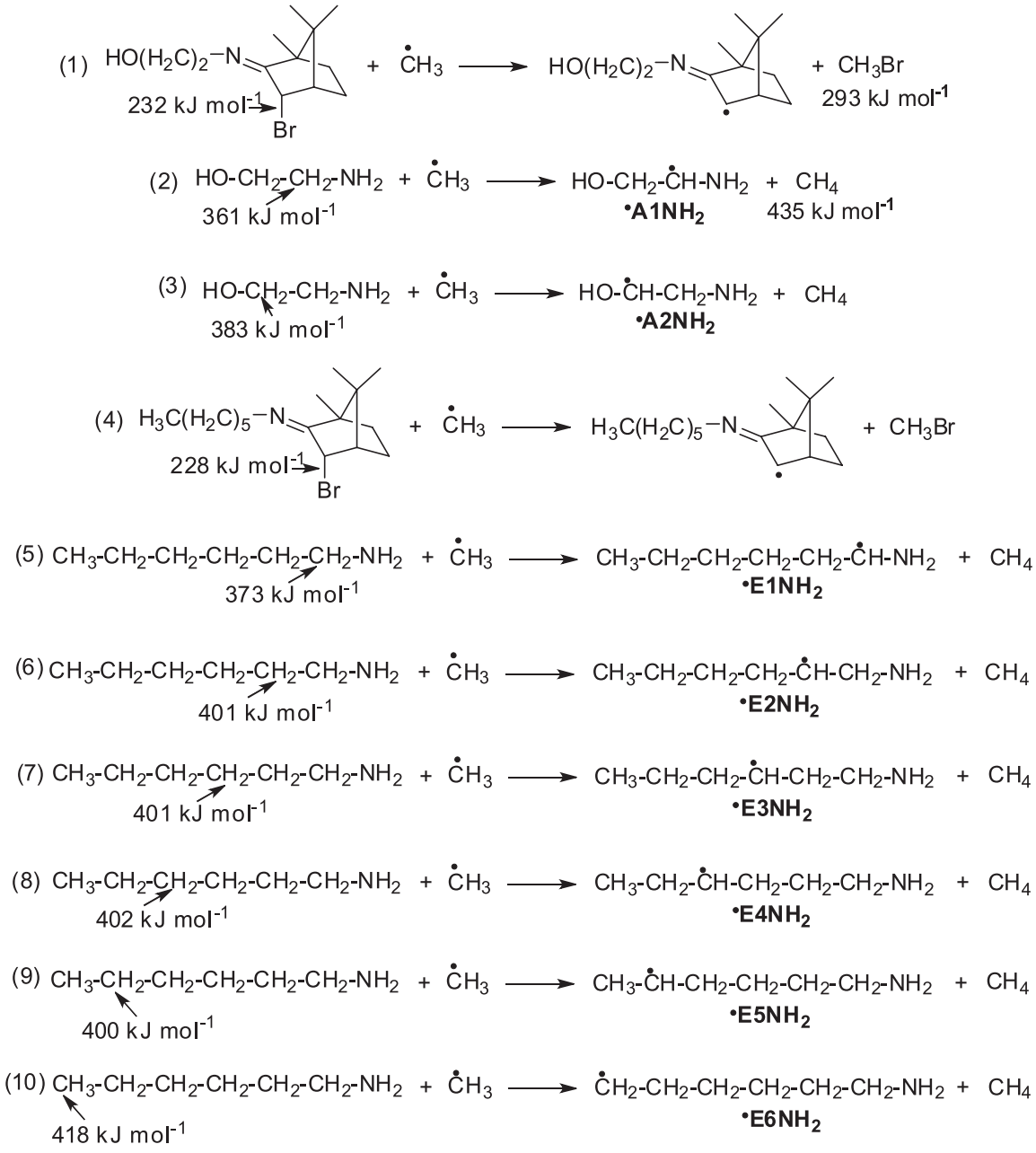

Figure 1. Isodesmic reactions used to estimate the C–Br and C–H bond dissociation enthalpies. The predicted values for all homolytic bond dissociation enthalpies are given.

isodesmic reactions at 298 K (25 °C) were constructed (Figure 1).

The homolytic dissociation enthalpies were calculated as follows:

$$\Delta H_{C\text{-}Br} = \Delta H_r + 293 \text{ kJ mol}^{-1} \quad (11)$$

$$\Delta H_{C\text{-}H} = \Delta H_r + 435 \text{ kJ mol}^{-1} \quad (12)$$

In equations 11 and 12, ΔH_{C-Br} and ΔH_{C-H} stand for the homolytic dissociation enthalpies of the C–Br and C–H bonds, respectively, ΔH_r represents the calculated enthalpy of a given isodesmic reaction, 293 kJ mol^{-1} is the experimental value for the enthalpy of homolytic cleavage of the C–Br bond in methyl bromide, and 435 kJ mol^{-1} is the experimental value for the enthalpy of homolytic cleavage of the C–H bond in methane.[34] Both experimental enthalpies refer to the gas phase at 25 °C.

Results and Discussion

The secondary and tertiary amines are known as dehalogenating agents. The reduction of α-bromocamphor

has been reported to yield camphor in the presence of *N*,*N*-dimethylaniline at 200 °C.[35] The reduction can be affected at much lower temperatures in the presence of di-*tert*-butylperoxide in acetonitrile.[36] In the reaction of α-bromocamphor with *N*-methylaniline as a debrominating agent, hydrocarbon camphane, tricyclene and bornylaniline were formed.[37] However, an attempt to use primary amines as debrominating agents had never previously been reported in the literature. To the best of our knowledge, only ethanolamine gave *N*-(2-hydroxyethyl)camphanimine in the reaction with 3-bromocamphor, but in presence of copper as dehalogenating agent.[38] In addition, it is noteworthy to point out that condensation of camphor with primary amines requires long reaction time and high temperatures in order to achieve reasonable yields of the desired imines.[39,40] On the basis of our investigation of this synthetic methodology, here it is reported several representative examples of the synthesis of *N*-substituted camphanimines using α-bromocamphor as chiral bicyclic ketone precursor (Scheme 1).

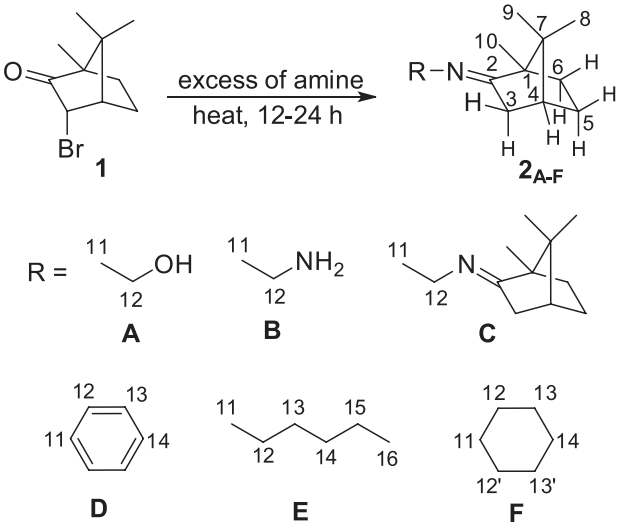

Scheme 1. Reductive debromination of *endo*-(+)-3-bromocamphor with some primary amines accompanied with imine formation.

Our initial research was focused on the study of solvents, temperature and 3-bromocamphor/ethanolamine molar ratio in order to establish the optimal reaction conditions for one-pot reductive debromination followed by Schiff base formation. After a number of attempts to perform the reaction in solvents of different polarity and boiling points, it was found that ethanolamine reacts only in refluxing xylene after 24 h giving the desired product in very low isolated yield (7%). However, in the absence of solvent, the reaction became facile, and after 12 h of heating at 130-135 °C (temp. of oil bath) imine $\mathbf{2}_A$ was isolated in 73% yield (Table 1). Due to poor solubility of 3-bromocamphor in ethanolamine and its partial sublimation, it was necessary to return it in the reaction flask mechanically from time to time. To overcome this problem, a Schlenk bomb was used to provide a closed reaction system. It is important to note that there was no significant difference in the yields, but the time required for the complete conversion of 3-bromocamphor was prolonged by additional 12 h. The molar ratio 3-bromocamphor/ethanolamine 1:10 was found to be optimal for this reaction. The decreasing of this ratio leads to extended reaction time while the increasing affords lower yields. With optimized reaction conditions, the debromination and imine formation were explored using primary amines with different polarities and boiling points. To successfully carry out this reaction, the superior results were obtained by selection of polar amine with sufficiently high boiling point in the role of reactant and solvent. For example, in comparison with *n*-hexylamine, as a consequence of the similar polarity but a lower boiling point, *n*-butylamine did not react with 3-bromocamphor even after extended time of heating.

The reaction of ethylene diamine also proceeded smoothly to afford products $\mathbf{2}_B$ and $\mathbf{2}_C$ in 47 and 29% yields, respectively. A better yield of $\mathbf{2}_B$ is possible to achieve by increasing of the amine/3-bromocamphor molar ratio. The absence of the desired debrominated product in reaction of 2-amino-2-methyl-1-propanol clearly suggests a crucial role of the substituent size for successful debromination of *endo*-(+)-3-bromocamphor. Aniline reacted with 3-bromocamphor only at elevated temperature leading to low yield of debrominated product (16%) together with camphor (11%), significant amount of diphenylamine and resinous material of undefined composition.

The compound $\mathbf{2}_A$ is selected as an illustrative example for the structure elucidation and ^{1}H and ^{13}C NMR assignments of all signals of the bicyclic skeleton. The downfield signal in the ^{1}H NMR spectrum (δ 2.35 ppm) must be $3H_a$ or $3H_e$ as a consequence of the proximity to the imino group. That it is $3H_e$ can be established by the connectivities in the correlation spectroscopy (COSY) spectrum in which this low field signal has three cross peaks which correspond to coupling to $3H_a$ (δ 1.84 ppm), 4H (δ 1.95 ppm) and $5H_e$ (δ 1.89 ppm). These assignments are confirmed by ^{1}H NMR signals for $3H_a$ and 4H. $3H_a$ is a doublet (J 17.00 Hz, geminal coupling), though coupling to the vicinal 4H might be expected. However, $3H_a$ and 4H showed absolutely no coupling, indicating a dihedral angle of approximately 90° between them. Similarly, the dihedral angle between 4H and $5H_a$ is approximately 90°, thus, this coupling constant is also 0 Hz.

Consequently, on the basis of two cross peaks in the COSY spectrum, 4H is only coupled to two ($3H_e$ and $5H_e$)

Table 1. Optimization of reaction conditions for the synthesis of camphanimine derivatives

Amine	3-BrC[a]/Amine molar ratio	time / h	Temperature / °C	Conversion of 3-BrC[b] / %	Products	Isolated yield / %
Ethanolamine	1:25	12	130-135[c]	> 99	$\mathbf{2}_A$	70[d]
Ethanolamine	1:10	12	130-135[c]	> 99	$\mathbf{2}_A$	73[d]
Ethylene diamine	1:25	12	reflux[e]	> 99	$\mathbf{2}_B$ and $\mathbf{2}_C$	79[f]
Ethylene diamine	1:10	12	reflux[e]	> 99	$\mathbf{2}_B$ and $\mathbf{2}_C$	76[g]
Aniline	1:10	12	130-135[h]	0	–	–
Aniline	1:10	24	170-175[h]	> 99	$\mathbf{2}_D$ [i]	16
n-Butylamine	1:10	36	reflux[j]	0	–	–
n-Hexylamine	1:10	24	reflux[k]	35	$\mathbf{2}_E$	26
Cyclohexylamine	1:10	24	reflux[l]	21	$\mathbf{2}_F$	14
AMP[m]	1:10	24	130-135[n]	0	–	–

[a]3-Bromocamphor; [b]determined by NMR; [c]temperature of oil bath, b.p. (amine) = 170 °C; [d]Schlenk bomb is used to provide a closed reaction system; [e]b.p. (amine) = 118 °C; [f]61% ($\mathbf{2}_B$) and 18% ($\mathbf{2}_C$); [g]47% ($\mathbf{2}_B$) and 29% ($\mathbf{2}_C$); [h]temperature of oil bath, b.p. (amine) = 184 °C; [i]11% of camphor was isolated. Large amount of diphenylamine was detected; [j]b.p. (amine) = 78 °C; [k]b.p. (amine) = 131-132 °C; [l]b.p. (amine) = 134 °C; [m]2-amino-2-methyl-1-propanol; [n]temperature of oil bath, b.p. (amine) = 165 °C.

of four neighbors and the signal is observed to be a triplet. In addition, a strong NOESY (nuclear Overhauser effect spectroscopy) cross peak was observed between $3H_e$ and C9 methyl protons at 0.75 ppm, whereas none of methyl groups gave NOESY cross peak with doublet at 1.84 ppm assigned to $3H_a$, confirming that dt at 2.35 ppm is on the *exo* face away from the *gem*-dimethyl bridge.

The quaternary carbon atoms C1 and C7 are assigned using DEPT (distortionless enhancement by polarization transfer), one-bond (HSQC) and long-range (HMBC) ^{1}H-^{13}C NMR correlation experiments. Both carbons at 47.05 and 53.75 ppm display HMBC correlations with all methyl protons but only signal at 47.05 ppm shows a strong correlation with $3H_a$ and weaker one with $6H_a$. In the ^{1}H, ^{15}N HMBC spectrum nitrogen shows strong couplings to C12 protons and $3H_a$ (–97.8 ppm in F_1 and 1.84 ppm in F_2) as well as one weak correlation with $3H_e$ (–97.8 ppm in F_1 and 2.35 ppm in F_2). Finally, the HMBC spectrum showed a strong three-bond correlation between C10 methyl protons and imino group.

An additional confirmation of the structure of $\mathbf{2}_A$ is provided by an X-ray analysis. Suitable crystals for X-ray measurements are obtained by fast cooling of the solution of $\mathbf{2}_A$ in hexane at –20 °C. An ORTEP presentation of $\mathbf{2}_A$ is given in Figure 2. The crystallographic data, the data collection parameters and the refinement parameters for compound $\mathbf{2}_A$ are summarized in Table 2. Selected molecular structural parameters and hydrogen bond geometrical parameters for $\mathbf{2}_A$ are given in Tables 3 and 4, respectively.

Our assumption for the most probable mechanism of the debromination of 3-bromocamphor is outlined in

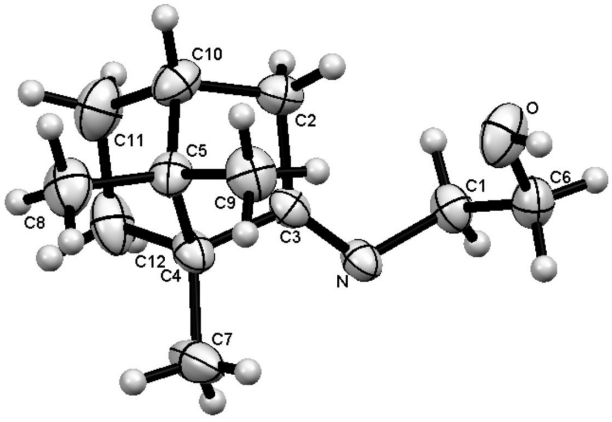

Figure 2. ORTEP type view of the asymmetric unit of $\mathbf{2}_A$ together with the atoms labeling scheme and displacement ellipsoids at the 50% probability level.

Scheme 2. Initially, 3-bromocamphor **1** adds one mole of primary amine to generate the intermediate Schiff base adduct $\mathbf{3}_R$. The ionic mechanism of debromination of 3-bromocamphor Schiff base $\mathbf{3}_R$ is not considered because the conventional literature mechanisms for typical S_N1, S_N2 or elimination reactions are not in accordance with the obtained experimental products. As a thermal decomposition of 3-bromocamphor itself at 200 °C yields only a small amount of camphor,[35] it is not reasonable to expect a homolytic cleavage of the C–Br bond and formation of free radicals at operating temperatures. In agreement with this reasoning is our numerous unsuccessful attempts to reveal a transition state for either homolytic cleavage of the C–Br bond in $\mathbf{3}_A$, or C–H bond in ethanolamine. However, a relevant number of initiating radicals ($\mathbf{I}^\bullet$ in Scheme 2) can be formed at these temperatures (but not at

Table 2. Selected crystallographic data for $\mathbf{2_A}$

Empirical formula	$C_{12}H_{21}NO$
M / (g mol^{-1})	195.3
Temperature / K	295
Wavelength / Å	0.71073
Crystal system	orthorhombic
Space group	$P2_12_12_1$
Unit cell dimensions / Å	a = 8.5206(6) b = 9.6686(5) c = 14.0849(9)
Volume / Å^3	1160.40 (13)
Mosaicity / degree	0.796(2)
Z	4
D_{calc} / (g mL^{-1})	1.115
Absorption coefficient / mm^{-1}	0.07
F(000)	432
Crystal size / mm	0.19 × 0.12 × 0.09
Color/Shape	colorless/prism
θ range / degree	3.55-24.99
Index ranges –h +h; –k +k; –l +l	–4 +10; –6 +11; –16 +16
Reflections collected	2804 (R_{int} = 0.0143)
Unique reflections	1919
Refinement methods	Full matrix L.S. on F^2
Data/restraints/parameters	1919/0/132
Goodness-of-fit on F^2	0.981
Final R indices [$F_o > 4\sigma F_o$]	R1 = 0.0406 (1789)
R indices (all unique data)	R1 = 0.0445, wR2 = 0.1133
Extinction coefficient	0.088(12)
Larg.diff. peak and hole / (e Å^{-3})	0.156 and –0.126

78 °C as it was found for *n*-butylamine) in the reactions of 3-bromocamphor or amine and reactive oxygen species generated by electron-transfer or energy-transfer processes. Hydroperoxides, like $RCH(NH_2)OOH$ formed in early stages of amine compound oxidation, decompose readily at ca. 120-130 °C giving reactive radical species.[41] Relevant to question of mechanism is the observation that reaction performed in a closed Schlenk apparatus requires a significantly longer time due to insufficient amount of oxygen gas in the system. It is reasonable to expect that these initiating radicals can trigger chain reactions leading to the products of the reactions of 3-bromocamphor with primary amines. According to the predicted bond dissociation enthalpies in Figure 1, C–H bonds in both amines are much stronger than C–Br bonds in the Schiff bases $\mathbf{3_A}$ and $\mathbf{3_E}$. If it is assumed that reactivity of $\mathbf{I}^{\bullet}$ towards present reactants ($\mathbf{3_R}$ or amine) is inversely proportional to the bond strengths, it turns out that the initiation reaction will be abstraction of $Br^{\bullet}$ from $\mathbf{3_R}$ by $\mathbf{I}^{\bullet}$, leading to the formation of radical $\mathbf{4_{R\bullet}}$. This radical abstracts $H^{\bullet}$ from the amine yielding the product $\mathbf{2_R}$ and radical $^{\bullet}RNH_2$, which further takes $Br^{\bullet}$ from $\mathbf{3_R}$, forming again radical $\mathbf{4_{R\bullet}}$ (Scheme 2). To confirm this assumption, the transformation of $\mathbf{3_A}$ and $\mathbf{3_E}$ was examined by means of density functional theory (DFT). Ethanolamine and *n*-hexylamine are selected as reactants with sufficiently high boiling points but of different polarity to possibly explain much lower yield of the reaction with *n*-hexylamine.

Table 3. Geometric parameters for $\mathbf{2_A}$

Bond length / Å		Bond angle / degree		Torsion angle / degree	
C1–C6	1.5135 (27)	C1–C6–O	109.80 (15)	C1–N–C3–C4	–178.97 (16)
C1–N	1.4710 (25)	C1–N–C3	118.41 (16)	C2–C3–C4–C5	–35.01 (17)
C2–C3	1.5190 (25)	C2–C3–N	129.83 (17)	C2–C3–C4–C7	–162.12 (16)
C2–C10	1.5289 (30)	C2–C10–C5	102.72 (14)	C2–C3–C4–C12	70.00 (18)
C3–C4	1.5188 (26)	C2–C10–C11	106.14 (16)	C2–C10–C11–C12	70.65 (20)
C3–N	1.2693 (24)	C3–C2–C10	102.35 (15)	C3–C2–C10–C5	35.09 (16)
C4–C5	1.5688 (25)	C3–C4–C5	100.39 (15)	C3–C2–C10–C11	–72.36 (18)
C4–C7	1.5211 (29)	C3–C4–C7	115.76 (17)	C4–C5–C10–C2	–54.82 (15)
C4–C12	1.5495 (28)	C3–C4–C12	104.21 (16)	C5–C10–C11–C12	–36.82 (20)
C5–C10	1.5454 (29)	C4–C5–C10	93.48 (14)	C5–C4–C3–N	144.99 (16)
C6–O	1.4090 (25)	C4–C12–C11	104.65 (16)	C8–C5–C10–C2	–173.30 (17)
C10–C11	1.5452 (29)	C5–C4–C12	101.70 (15)	C9–C5-C10-C2	62.32 (18)
C11–C12	1.5334 (36)	C5–C10–C11	102.70 (17)	C10–C2–C3–N	–179.49 (18)
		C6–C1–N	111.88 (15)	C12–C4–C3–N	–109.99 (20)
		C7–C4–C12	115.43 (17)	N–C1–C6–O	–70.31 (20)
		C10–C11–C12	102.80 (17)	C1–N–C3–C4	–178.97 (16)

Table 4. Hydrogen-bond geometry for $\mathbf{2_A}$

D—H···*A*	*D*—H / Å	H···*A* / Å	*D*···*A* / Å	*D*—H···*A* /degree
O—H0···N^{i}	0.82	2.02	2.837	170.83

Symmetry codes: (i) –x + 1, y + 1/2, –z + 3/2.

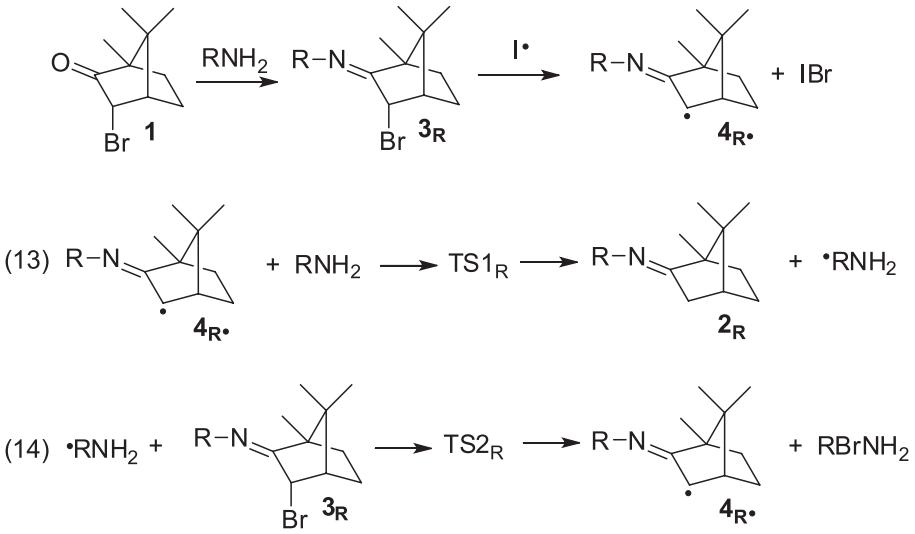

Scheme 2. A suggested mechanism for reductive debromination followed by imine formation.

In the step 13 with ethanolamine, hydrogen atom can be abstracted from C11 or C12 (Scheme 1), implying that two radicals can be produced: $^{\bullet}A1NH_2$ or $^{\bullet}A2NH_2$ (Figure 1). Similarly, six radicals ($^{\bullet}E1NH_2$ - $^{\bullet}E6NH_2$) can be formed upon abstraction of hydrogen atom from different carbons of *n*-hexylamine. In this work, abstraction of hydrogen from both C11 and C12 of ethanolamine as well as from C11 and C13 of *n*-hexylamine were examined. Note that C11–H is the weakest C–H bond in both amines (Figure 1). In addition, all corresponding pathways 14 were investigated. The revealed transition states are presented in Figure 3, whereas the optimized geometries of corresponding reactants and products are depicted in the Supplementary Information (SI) section. In Table 5, the relevant relative free energies, as well as activation enthalpies and entropy terms, are listed.

The NBO analysis of $\mathbf{4_{R\bullet}}$ shows that the unpaired electron is delocalized between C3 and imine nitrogen. In $\mathbf{TS1_R}$ (Figure 3), a C–H bond in amine is being cleaved, whereas the C3–H bond is being formed. Step 13 yields the product of the overall reaction $\mathbf{2_R}$ and an amine radical. Due to the vicinity of electron donating amino group which stabilizes electron deficient C11, $^{\bullet}\mathbf{A1NH_2}$ is by 21.1 kJ mol^{-1} more stable than $^{\bullet}\mathbf{A2NH_2}$, and $^{\bullet}\mathbf{E1NH_2}$ is by 24.0 kJ mol^{-1} more stable than $^{\bullet}\mathbf{E3NH_2}$. As a consequence, abstraction of hydrogen from C11 of both amines is less endothermic (Table 5). A radical formed in step 13 abstracts bromine atom from $\mathbf{3_R}$ via transition state $\mathbf{TS2_R}$. In $\mathbf{TS2_R}$, a simultaneous cleavage of the C3–Br bond in $\mathbf{3_R}$ and formation of the bond between bromine and corresponding carbon in $^{\bullet}\mathbf{RNH_2}$ occur. Elementary step 14 is exothermic, and yields a bromide and radical $\mathbf{4_{R\bullet}}$ which is again involved in step 13, thus propagating the chain reaction.

In all transition states, spin density is distributed among C3, imine nitrogen and corresponding carbon of the amine. In transition states with ethanolamine, delocalization of the unpaired electron also involves the amine oxygen. In addition, in transition states involving C11, significant spin density values on the nitrogen of the amino group were observed. Due to better delocalization of the unpaired electron, transition states with ethanolamine require lower activation barriers in comparison with those with *n*-hexylamine. Similarly, transition states involving C11 require lower activation barriers in comparison with those involving C12 and C13 (Table 2).

Table 5 shows that activation energies are in general proportional to the predicted bond strengths (Figure 1), i.e., activation barriers for abstraction of hydrogen are much higher than those for abstraction of bromine. These findings confirm our assumption of initial formation of $\mathbf{4_{R\bullet}}$ radical. Furthermore, since all C–H bonds in *n*-hexylamine are stronger than C11–H, it is reasonable to expect that only abstraction of hydrogen from C11 will be energetically favored. In addition, step 14 is entropy-controlled ($\Delta H^{\ddagger}_{a} < -T\Delta S^{\ddagger}_{a}$). This finding implies that the rate of step 14 is predominantly governed by the issues of orientation, trajectory, accessibility, etc. All these

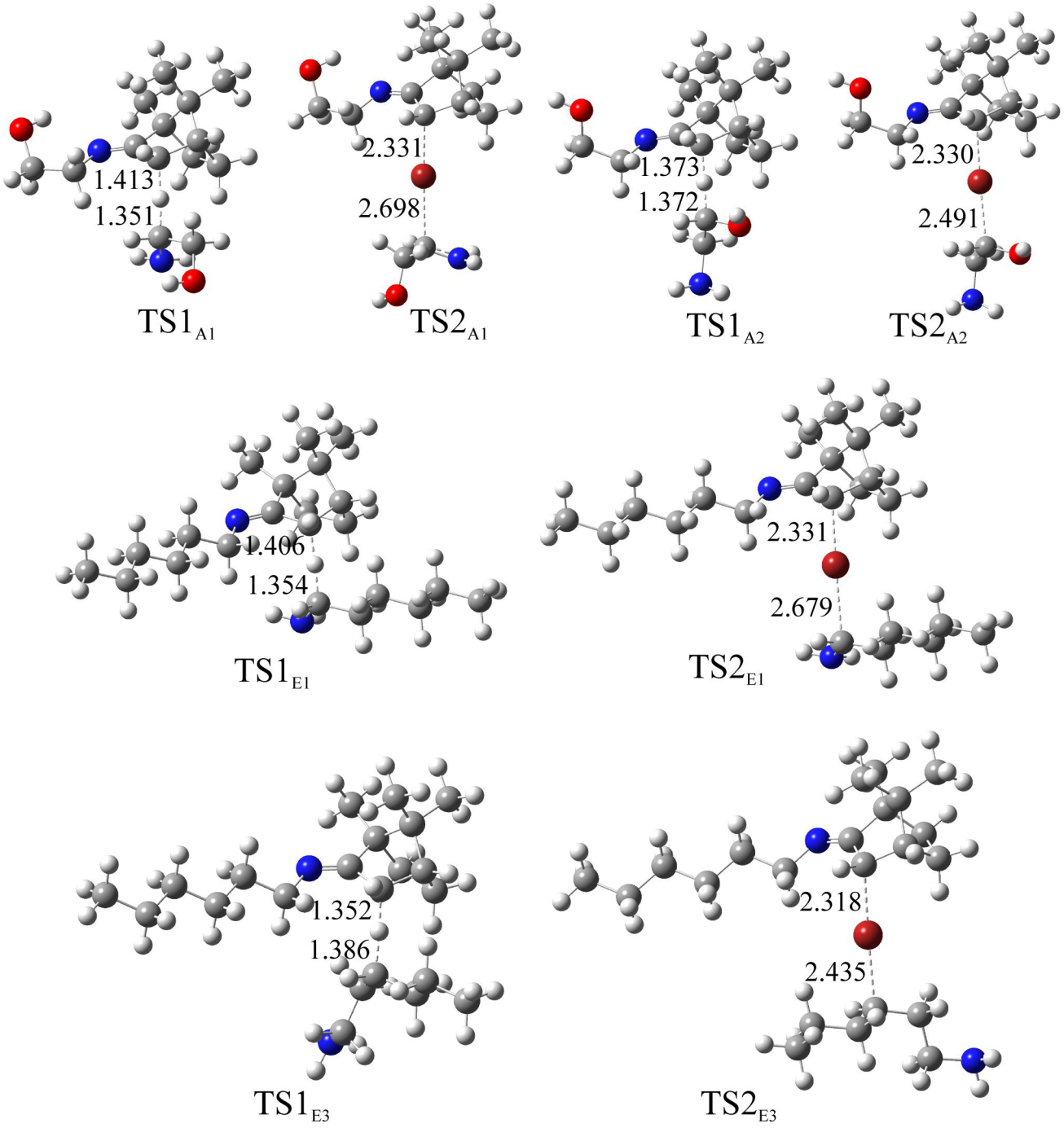

Figure 3. Transition states in elementary reactions 13 and 14 with crucial bond distances (Å) indicated.

facts indicate that only small fraction of intermolecular collisions in the reaction with *n*-hexylamine is successful at the experimental temperature, which leads to the low reaction yield.

The solvents can often have an important role on the rate of many radical reactions.[42] The rate constant for hydrogen abstraction from amine substrate by alkoxyl radicals was strongly affected by the solvent polarity.[43] It was found that abstraction rate constant dramatically depends on the solvent dielectric constant. Indeed, the conversion of 3-bromocamphor to the corresponding debrominated imine in the reaction with *n*-hexylamine (amine appears as a solvent and reactant) was much lower (only 35% after 24 h and 26% of isolated product). Polar ethanolamine and ethylenediamine stabilize polar transition states better than less polar *n*-hexylamine and provide the delocalization of the nitrogen lone pair in the α-hydrogen abstraction from the amine more successfully. As a consequence of

Table 5. Activation parameters: enthalpies ($\Delta H^{\ddagger}_{a}$), entropy terms ($-T\Delta S^{\ddagger}_{a}$), and free energies ($\Delta G^{\ddagger}_{a}$); and reaction free energies (ΔG_{r}) in elementary steps 13 and 14

Reaction step	$\Delta H^{\ddagger}_{a}$ / (kJ mol^{-1})	$-T\Delta S^{\ddagger}_{a}$ / (kJ mol^{-1})	$\Delta G^{\ddagger}_{a}$ / (kJ mol^{-1})	$\Delta G^{\ddagger}_{r}$ / (kJ mol^{-1})
$\mathbf{4_A}\cdot + HO(CH_2)_2NH_2 \rightarrow \mathbf{2_A} + \cdot\mathbf{A1NH_2}$	68.3	65.9	134.2	5.4
$\cdot\mathbf{A1NH_2} + \mathbf{3_A} \rightarrow \mathbf{4_A}\cdot + HOCH_2CHBr_NH2$	12.8	60.1	72.9	–59.4
Overall reaction			134.2	–54.0
$\mathbf{4_A}\cdot + HO(CH_2)_2NH_2 \rightarrow \mathbf{2_A} + \cdot\mathbf{A2NH_2}$	81.4	61.6	143.1	26.5
$\cdot\mathbf{A2NH_2} + \mathbf{3_A} \rightarrow \mathbf{4_A}\cdot + HOCHBrCH_2NH_2$	23.7	58.5	82.2	–56.5
Overall reaction			143.1	–30.0
$\mathbf{4_E}\cdot + CH_3(CH_2)_5NH_2 \rightarrow \mathbf{2_E} + \cdot\mathbf{E1_NH2}$	76.6	66.8	143.4	6.0
$\cdot\mathbf{E1NH_2} + \mathbf{3_E} \rightarrow \mathbf{4_E}\cdot + CH_3(CH_2)_4CHBrNH_2$	11.6	57.9	69.5	–69.0
Overall reaction			143.4	–63.0
$\mathbf{4_E}\cdot + CH_3(CH_2)_5NH_2 \rightarrow \mathbf{2_E} + \cdot\mathbf{E3NH_2}$	101.0	65.4	166.4	30.0
$\cdot\mathbf{E3NH_2} + \mathbf{3_E} \rightarrow \mathbf{4_E}\cdot + CH_3(CH_2)_2CHBr(CH_2)_2NH_2$	35.6	62.2	97.8	–53.3
Overall reaction			166.4	–23.3

increasing steric bulk of cyclohexylamine reactant, the yield of isolated imine was even lower (21% of 3-bromocamphor conversion and 14% of isolated imine product). The fact that *n*-butylamine does not react with 3-bromocamphor even after 36 h can be attributed to the insufficiently high reaction temperature (b.p. of *n*-butylamine = 78 °C) for generation of reactive radical species.

Conclusion

Our group found that ethanolamine and ethylene diamine can serve as efficient reagents for the one-step imine formation and effective reductive debromination of 3-bromocamphor. Although this reaction is also limited by steric factors, solvent polarity and boiling point of applied amine strongly influence the yields of the debrominated products. These findings are in accord with our DFT based investigation of the radical reaction mechanism with ethanolamine and *n*-hexylamine. It was found that the reaction with more polar ethanolamine is energetically more favorable. The entropy-controlled abstraction of the bromine atom from the Schiff base also contributes to the lower yield of the reaction with *n*-hexylamine.

Supplementary Information

Supplementary data (IR and NMR spectra, spectral data, experimental and calculated geometrical parameters of $\mathbf{2_A}$, optimized geometries of the reactants and products in the reactions with ethanolamine and *n*-hexylamine, and results of the IRC calculations for the corresponding transition states) are available free of charge at http://jbcs.sbq.org.br as a PDF file.

Acknowledgments

The authors are grateful to the Ministry of Science and Technological Development of the Republic of Serbia for financial support (Grant No. 172016).

References

1. Borowitz, I. J.; Grossman, L. I.; *Tetrahedron Lett.* **1962**, *3*, 471.
2. Ho, T. L.; Wong, C. M.; *J. Org. Chem.* **1974**, *39*, 562.
3. Alper, H.; Pattee, L.; *J. Org. Chem.* **1979**, *44*, 2568.
4. Olah, G. A.; Arvanaghi, M.; Vankar, Y. D.; *J. Org. Chem.* **1980**, *45*, 3531.
5. Kamiya, N.; Tanmatu, H.; Ishii, Y.; *Chem. Lett.* **1992**, *21*, 293.
6. Sayama, S.; Inamura, Y.; *Chem. Lett.* **1996**, *25*, 633.
7. Miura, Y.; Oka, H.; Yamano, E.; Morita, M.; *J. Org. Chem.* **1997**, *62*, 1188.
8. Kuivila, H. G.; Menapace, L. W.; *J. Org. Chem.* **1963**, *28*, 2165.
9. Sauers, R. R.; Hu, C. K.; *J. Org. Chem.* **1971**, *36*, 1153.
10. Ho, T. L.; Wong, C. M.; *Synth. Commun.* **1973**, *3*, 237.
11. Osuka, A.; Suzuki, H.; *Chem. Lett.* **1983**, *12*, 119.
12. Sarma, J. C.; Borbaruah, M.; Sharma, R. P.; *Tetrahedron Lett.* **1985**, *26*, 4657.
13. Nishiyama, Y.; Katsuen, S.; Jounen, H.; Hamanaka, S.; Ogawa, A.; Sonoda, N.; *Heteroat. Chem.* **1990**, *1*, 467.
14. Chung, S. K.; Hu, Q. Y.; *Synth. Commun.* **1982**, *12*, 261.
15. Denis, J. N.; Krief, A.; *Tetrahedron Lett.* **1981**, *22*, 1431.
16. Ranu, C. B.; Chattopadhyay, K.; Jana, R.; *Tetrahedron* **2007**, *63*, 155.
17. Squire, M. D.; Burwell, A.; Ferrence, G. M.; Hitchcock, S. R.; *Tetrahedron: Asymmetry* **2002**, *13*, 1849.
18. Heiden, Z. M.; Stephan, D. W.; *Chem. Commun.* **2011**, *47*, 5729.

19. Gavrilov, K.; Tsarev, V.; Zheglov, S.; Korlyukov, A.; Antipin, M.; Davankov, V.; *Synthesis* **2007**, *11*, 1717.
20. *Data Collection and Processing Software*, version 1; Oxford Diffraction Ltd, UK, 2006.
21. *CrysAlisPro*, Oxford Diffraction Ltd. (2010). Version 1.171.34.36 (release 02-08-2010 CrysAlis171 .NET).
22. Wilson, A. J. C.; *International Tables for X-ray Crystallography*, vol. C; Kluwer Academic Publishers: Dordrecht, 1992, p. 500-502, 219-222, 193-199.
23. Altomare, A.; Gascarano, G.; Giacovazzo, C.; Guagliardi, A.; *J. Appl. Crystallogr.* **1993**, *26*, 343.
24. Macrae, C. F.; Bruno, I. J.; Chisholm, J. A.; Edgington, P. R.; McCabe, P.; Pidcock, E.; Rodriguez-Monge, L.; Taylor, R.; van de Streek, J.; Wood, P. A.; *J. Appl. Crystallogr.* **2008**, *41*, 466.
25. Sheldrick, G.; *SHELXL-97 Program for Crystal Structure Refinement*; Institüt für Anorganische Chemie der Universität, Tammanstrasse 4, D-3400 Gottingen, Germany, 1997.
26. Frisch, M. J.; Trucks, G. W.; Schlegel, H. B.; Scuseria, G. E.; Robb, M. A.; Cheeseman, J. R.; Scalmani, G.; Barone, V.; Mennucci, B.; Petersson, G. A.; Nakatsuji, H.; Caricato, M.; Li, X.; Hratchian, H. P.; Izmaylov, A. F.; Bloino, J.; Zheng, G.; Sonnenberg, J. L.; Hada, M.; Ehara, M.; Toyota, K.; Fukuda, R.; Hasegawa, J.; Ishida, M.; Nakajima, T.; Honda, Y.; Kitao, O.; Nakai, H.; Vreven, T.; Montgomery Jr., J. A.; Peralta, J. E.; Ogliaro, F.; Bearpark, M.; Heyd, J. J.; Brothers, E.; Kudin, K. N.; Staroverov, V. N.; Kobayashi, R.; Normand, J.; Raghavachari, K.; Rendell, A.; Burant, J. C.; Iyengar, S. S.; Tomasi, J.; Cossi, M.; Rega, N.; Millam, J. M.; Klene, M.; Knox, J. E.; Cross, J. B.; Bakken, V.; Adamo, C.; Jaramillo, J.; Gomperts, R.; Stratmann, R. E.; Yazyev, O.; Austin, A. J.; Cammi, R.; Pomelli, C.; Ochterski, J. W.; Martin, R. L.; Morokuma, K.; Zakrzewski, V. G.; Voth, G. A.; Salvador, P.; Dannenberg, J. J.; Dapprich, S.; Daniels, A. D.; Farkas, O.; Foresman, J. B.; Ortiz, J. V.; Cioslowski, J.; Fox, D. J.; *Gaussian 09*, *Rev A.02*, Gaussian Inc., Wallingford, 2009.
27. Lee, C.; Yang, W.; Parr, R. G.; *Phys. Rev. B: Condens. Matter Mater. Phys.* **1988**, *37*, 785.
28. Becke, A. D.; *J. Chem. Phys.* **1993**, *98*, 5648.
29. Ikada, E.; Hida, Y.; Okamoto, H.; Hagino, J.; Koizumi, N.; *Bull. Inst. Chem. Res., Kyoto Univ.* **1968**, *46*, 239.
30. Sild, S.; Karelson, M.; *J. Chem. Inf. Comput. Sci.* **2002**, *42*, 360.
31. Cossi, M.; Rega, N.; Scalmani, G.; Barone, V.; *J. Comput. Chem.* **2003**, *24*, 669.
32. Foster, J. P.; Weinhold, F.; *J. Am. Chem. Soc.* **1980**, *102*, 7211.
33. Glendening, E. D.; Badenhoop, J. K.; Reed, A. E.; Carpenter, J. E.; Bohmann, J. A.; Morales, C. M.; Weinhold, F.; *GenNBO 5.0*; Theoretical Chemistry Institute, University of Wisconsin, Madison, 2001.
34. Srivastava, A. K.; *Organic Chemistry Made Simple*; New Age International (P) Ltd.: New Delhi, India, 2002.
35. Giumanini, A. G.; Musiani, M. M.; *Z. Naturforsch.* **1977**, *32B*, 1314.
36. Chen, J. J.; Tanner, D. D.; *Can. J. Chem.* **1992**, *70*, 173.
37. Giumanini, A. G.; Musiani, M. M.; *J. Prakt. Chem.* **1980**, *322*, 423.
38. Wei, L.; Steck, E. A.; *Can. J. Chem.* **1964**, *42*, 2623.
39. Love, B. F.; Ren, J.; *J. Org. Chem.* **1993**, *58*, 5556.
40. Taguchi, K.; Westheimer, F. H.; *J. Org. Chem.* **1971**, *36*, 1570.
41. Frimer, A. A.; Aljadeff, G.; Ziv, J.; *J. Org. Chem.* **1983**, *48*, 1700.
42. Litwinienko, G.; Beckwith, A. L. J.; Ingold, K. U.; *Chem. Soc. Rev*. **2011**, *40*, 2157.
43. Encinas, M. V.; Diaz, S.; Lissi, E.; *Int. J. Chem. Kinet.* **1981**, *13*, 119.

Submitted: February 12, 2013
Published online: June 7, 2013

J. Braz. Chem. Soc., Vol. 24, No. 7, S1-S17, 2013.
Printed in Brazil - ©2013 Sociedade Brasileira de Química
0103 - 5053 $6.00+0.00

Supplementary Information

Debromination of *endo*-(+)-3-Bromocamphor with Primary Amines

Svetlana Marković,[a] Violeta Marković,[a] Milan D. Joksović,[a] Nina Todorović,[b] Ljubinka Joksović,*,[a] Vladimir Divjaković[c] and Snežana Trifunović[d]

[a]Department of Chemistry, Faculty of Science, University of Kragujevac, 12 R. Domanovića, 34000 Kragujevac, Serbia

[b]Institute for Chemistry, Technology and Metallurgy, 12 Njegoševa, 11000 Belgrade, Serbia

[c]Department of Physics, University of Novi Sad, 3 Trg D.Obradovića, 21000 Novi Sad, Serbia

[d]Faculty of Chemistry, University of Belgrade, 16 Trg Studentski, PO Box 158, 11000 Belgrade, Serbia

IR spectra of $\mathbf{2}_{\mathbf{A\text{-}F}}$

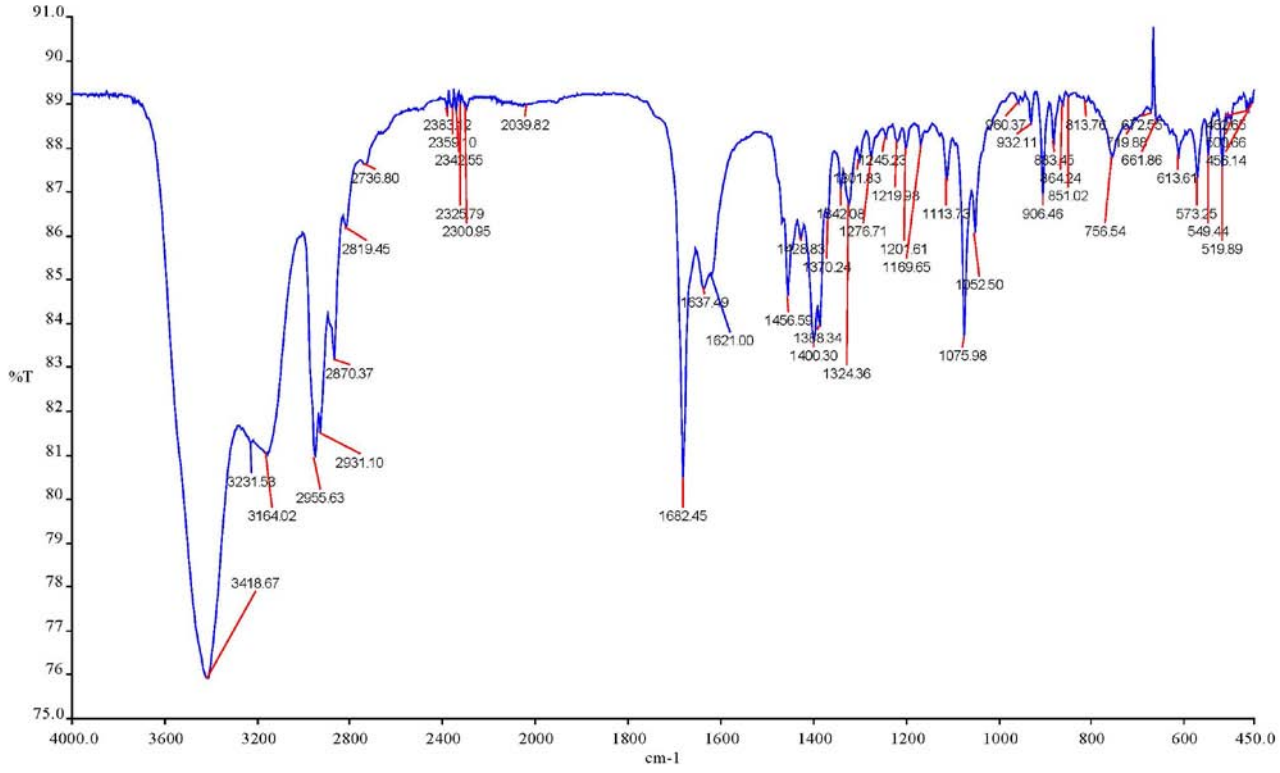

Figure S1. IR spectrum of $\mathbf{2}_{\mathbf{A}}$ (KBr disc).

*e-mail: ljubinka@kg.ac.rs

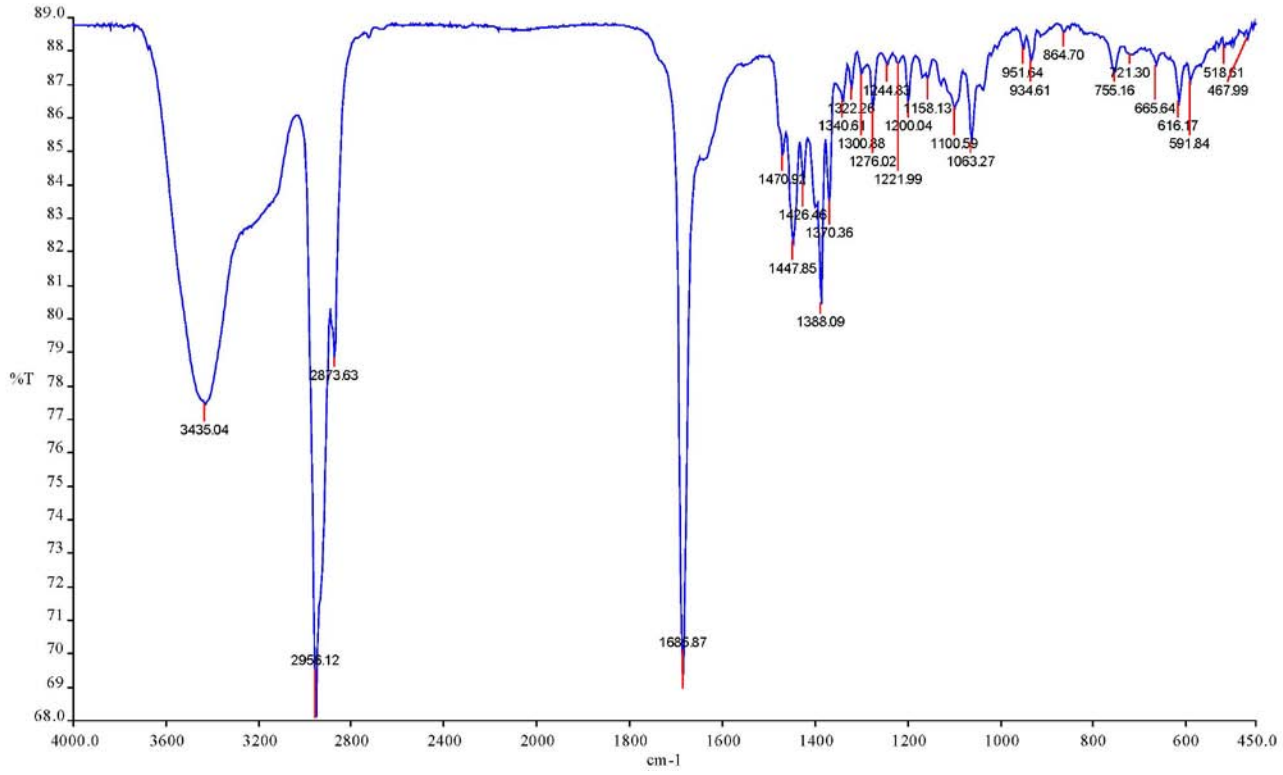

Figure S2. IR spectrum of $\mathbf{2_B}$ (KBr disc).

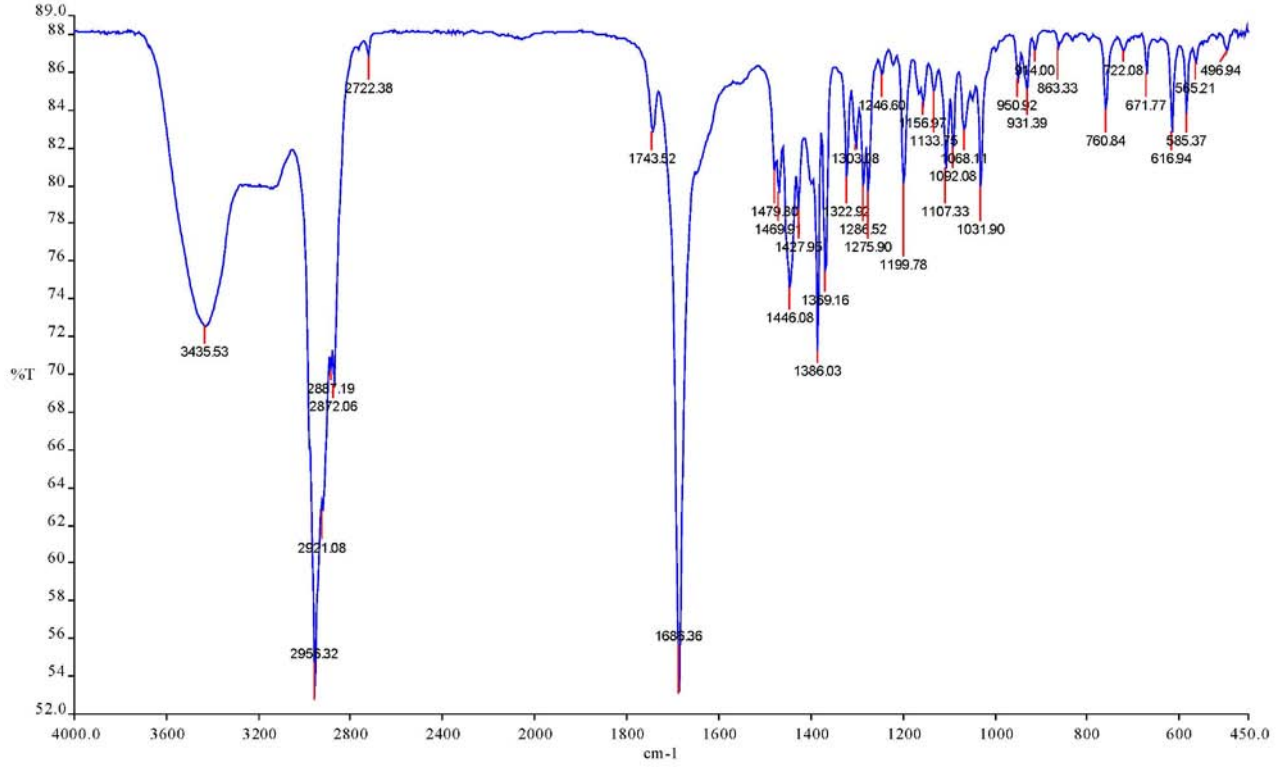

Figure S3. IR spectrum of $\mathbf{2_C}$ (KBr disc).

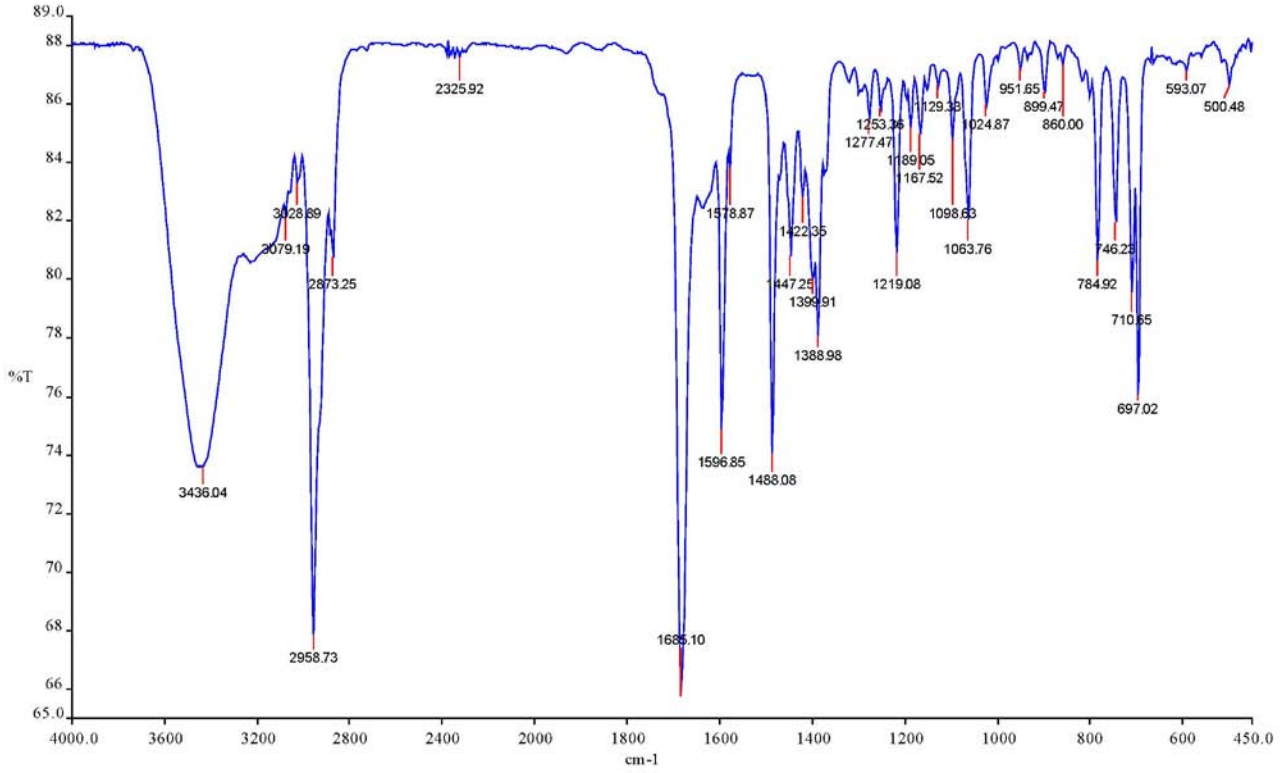

Figure S4. IR spectrum of $\mathbf{2}_{\mathbf{D}}$ (neat).

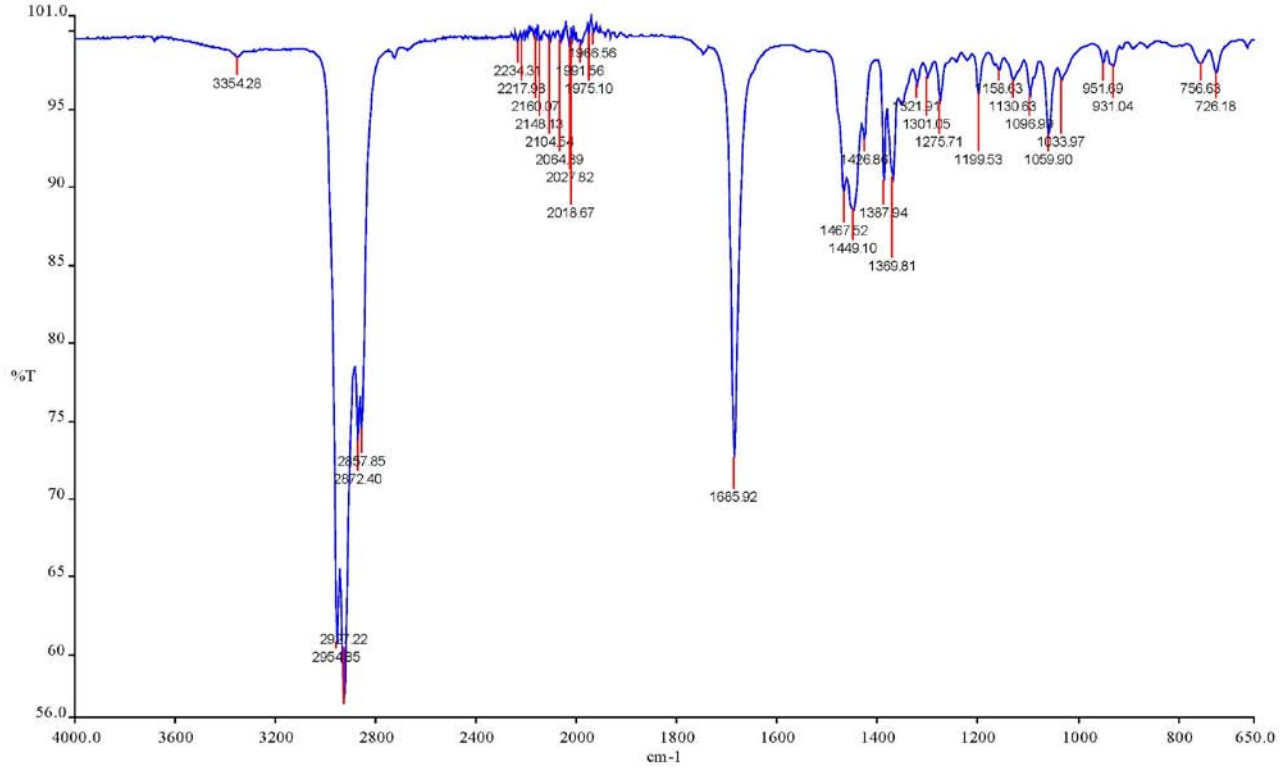

Figure S5. IR spectrum of $\mathbf{2}_{\mathbf{E}}$ (neat).

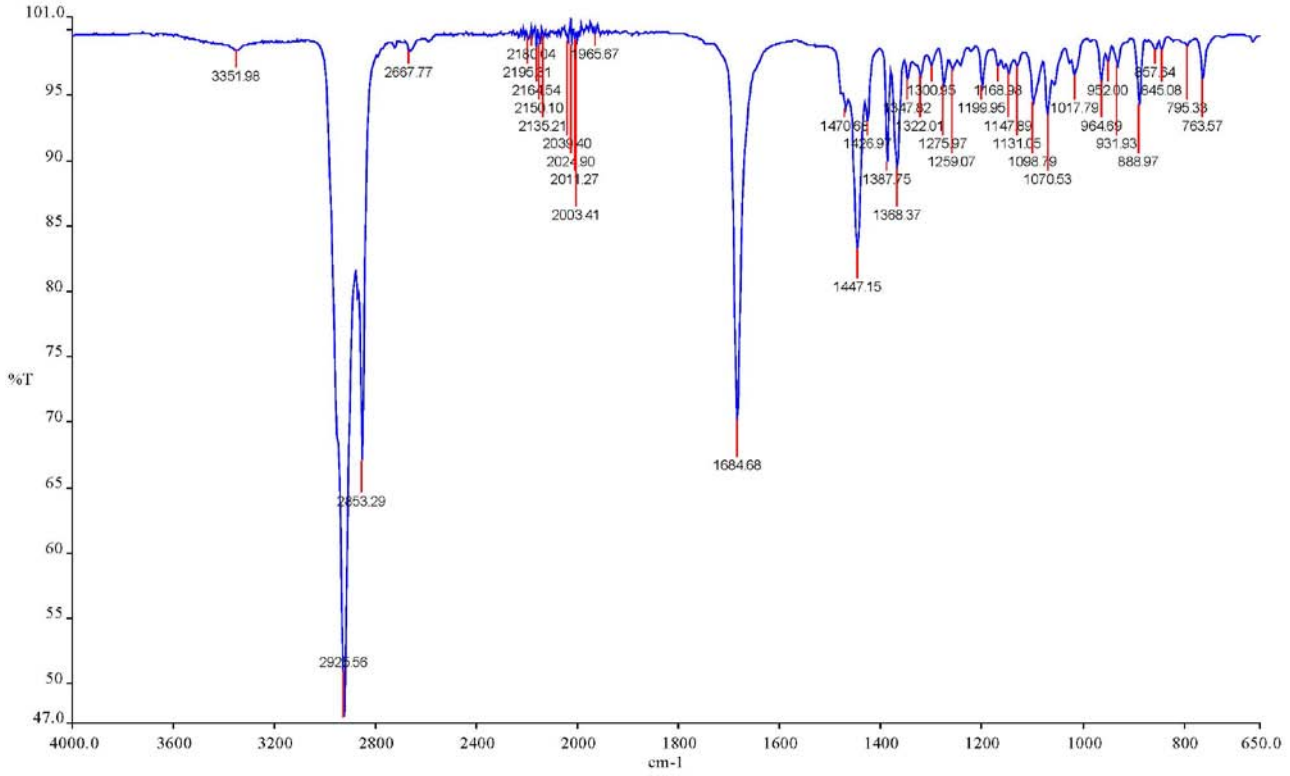

Figure S6. IR spectrum of $\mathbf{2}_{F}$ (neat).

NMR spectra of $\mathbf{2}_{A\text{-}F}$

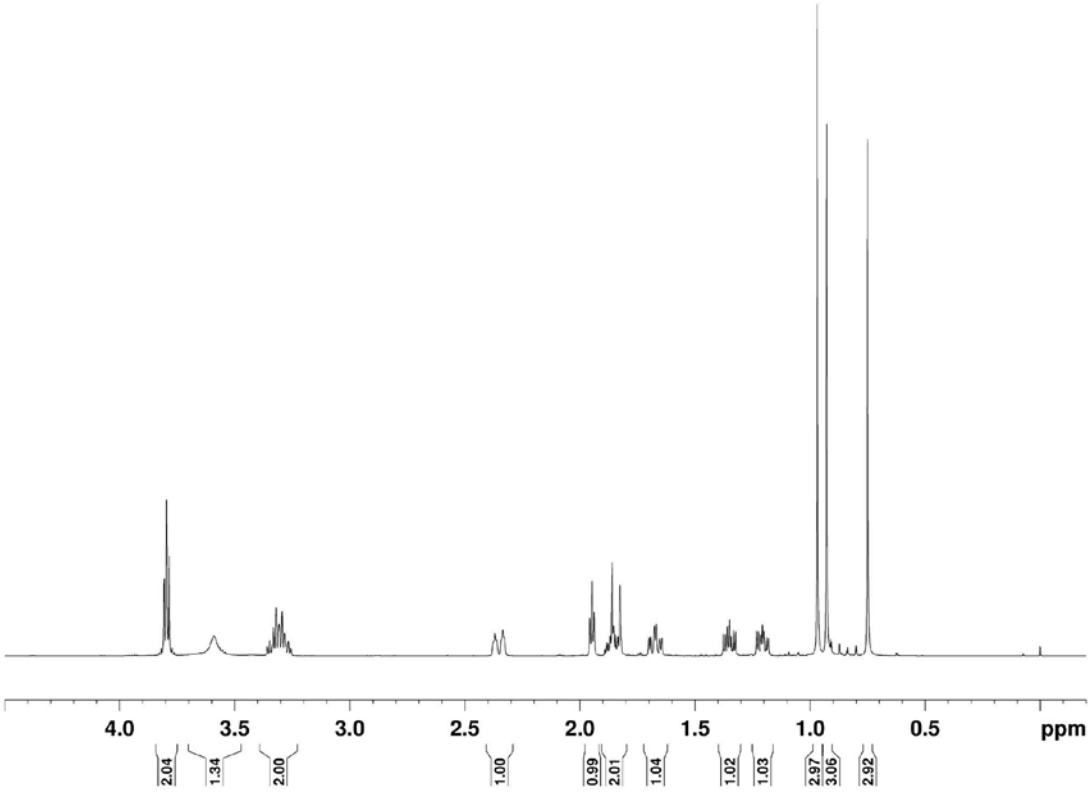

Figure S7. ^{1}H NMR spectrum of $\mathbf{2}_{A}$ ($CDCl_3$, 500 MHz).

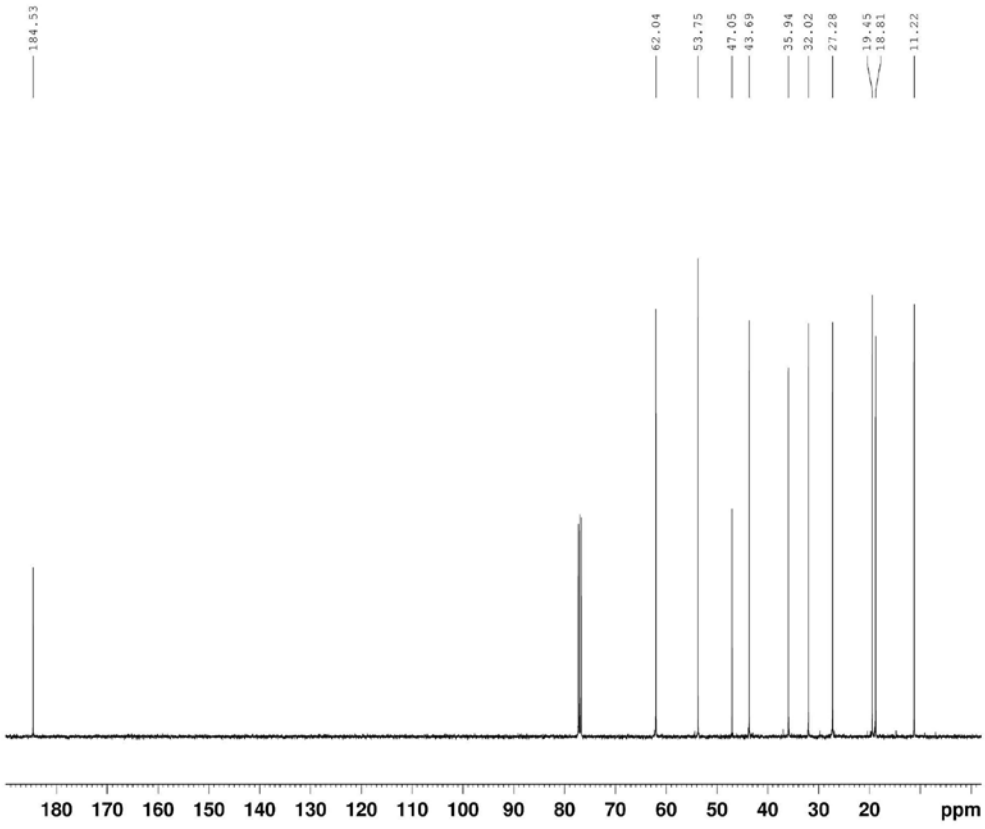

Figure S8. ^{13}C NMR spectrum of $\mathbf{2_A}$ ($CDCl_3$, 125 MHz).

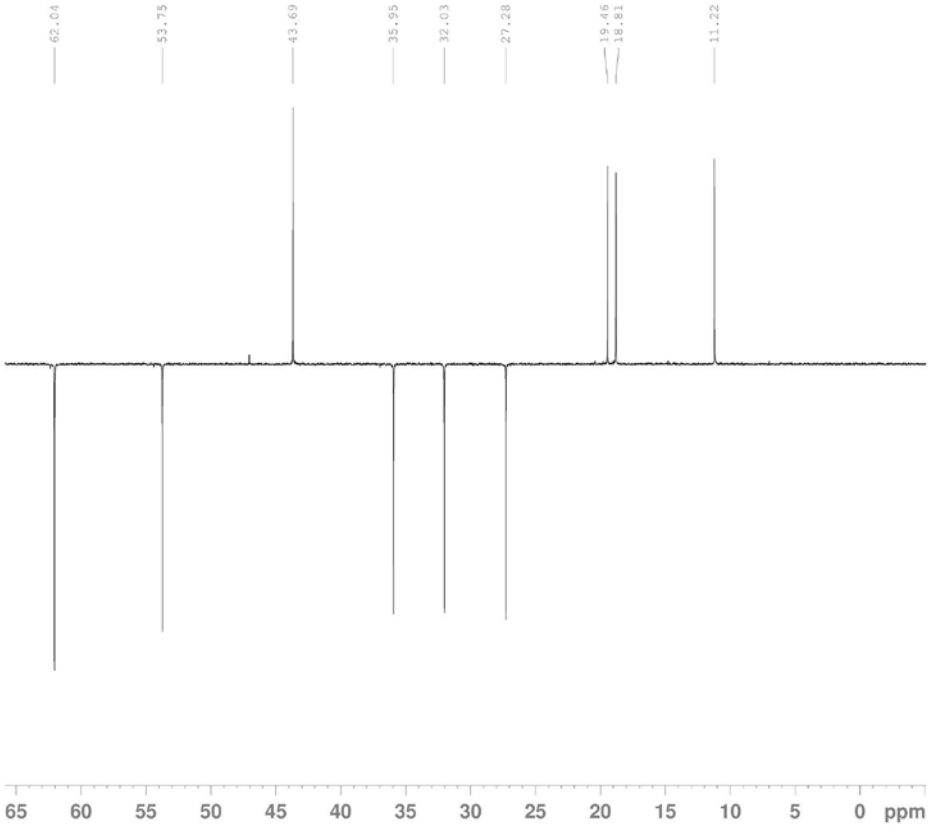

Figure S9. DEPT spectrum of $\mathbf{2_A}$ ($CDCl_3$, 125 MHz).

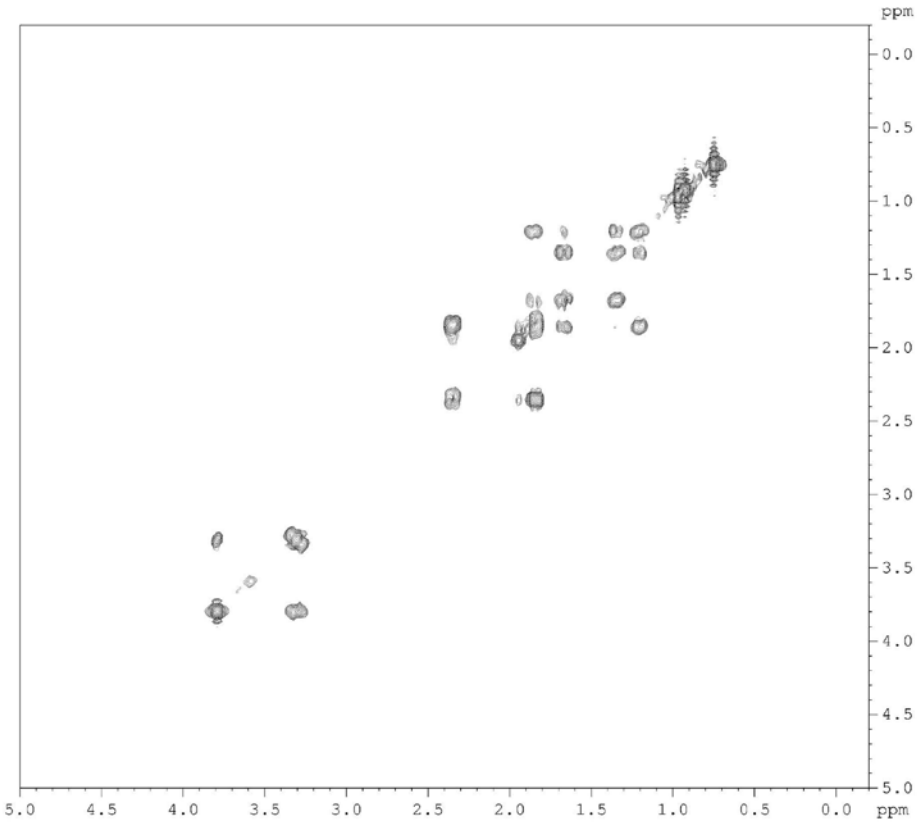

Figure S10. COSY spectrum of $\mathbf{2_A}$ ($CDCl_3$, 500 MHz).

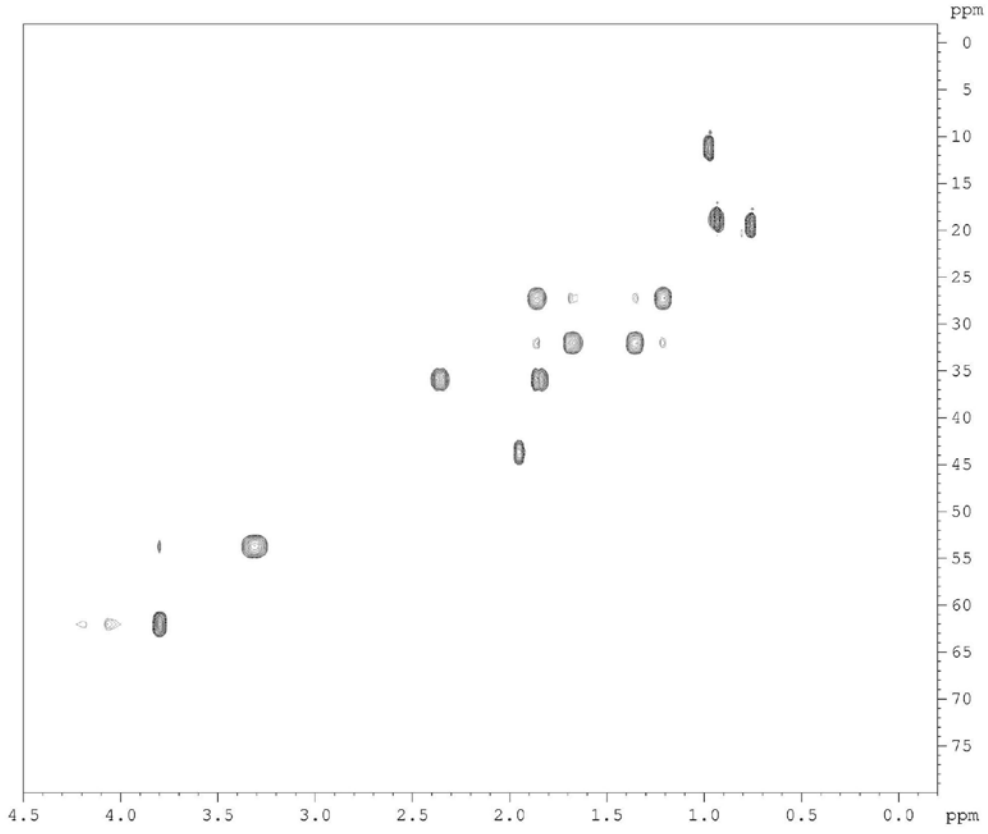

Figure S11. HSQC spectrum of $\mathbf{2_A}$ ($CDCl_3$, 500 MHz).

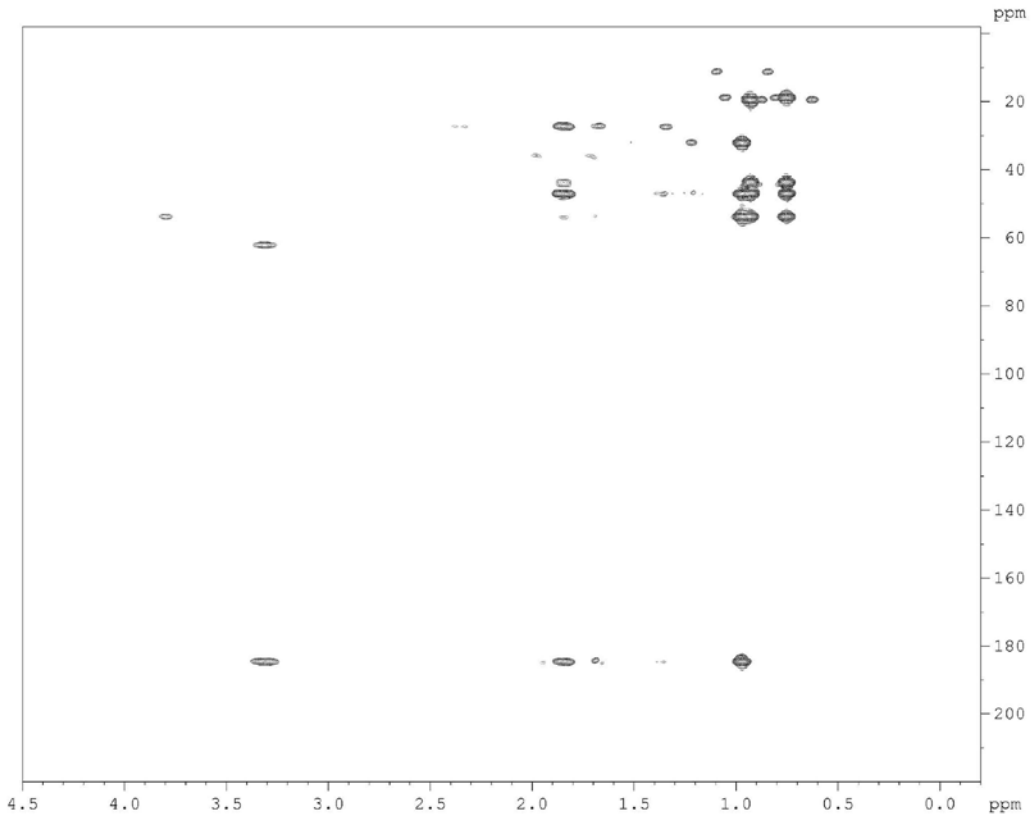

Figure S12. HMBC spectrum of $\mathbf{2}_{\mathbf{A}}$ ($CDCl_3$, 500 MHz).

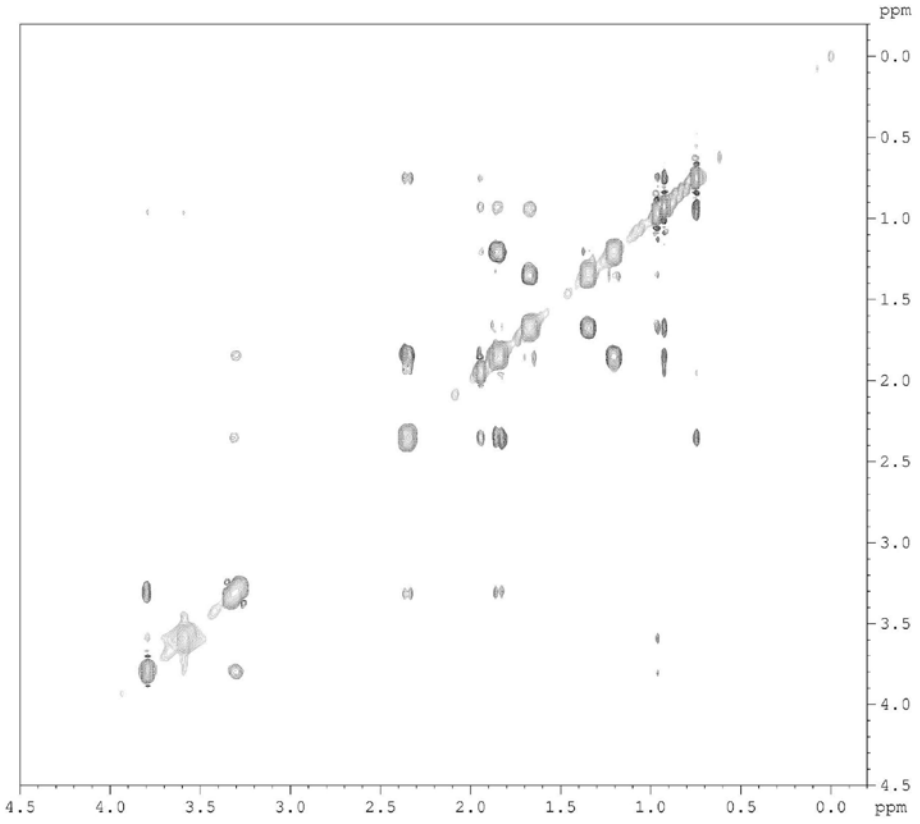

Figure S13. NOESY spectrum of $\mathbf{2}_{\mathbf{A}}$ ($CDCl_3$, 500 MHz).

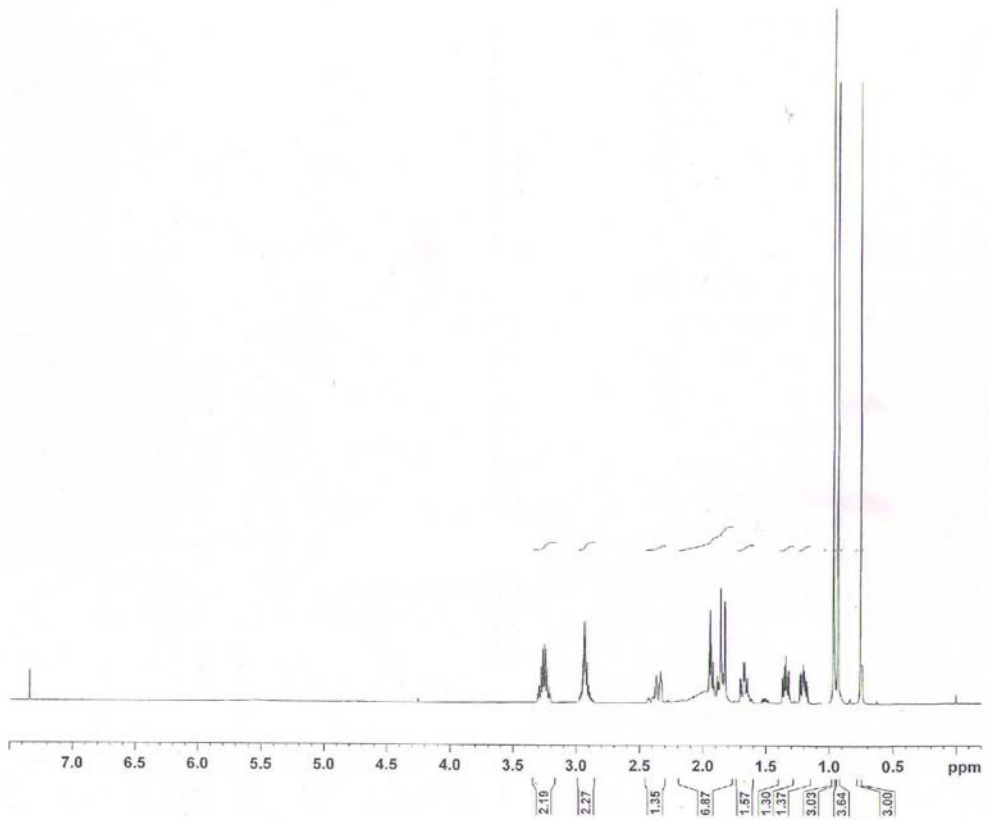

Figure S14. [1]H NMR spectrum of $\mathbf{2_B}$ ($CDCl_3$, 500 MHz).

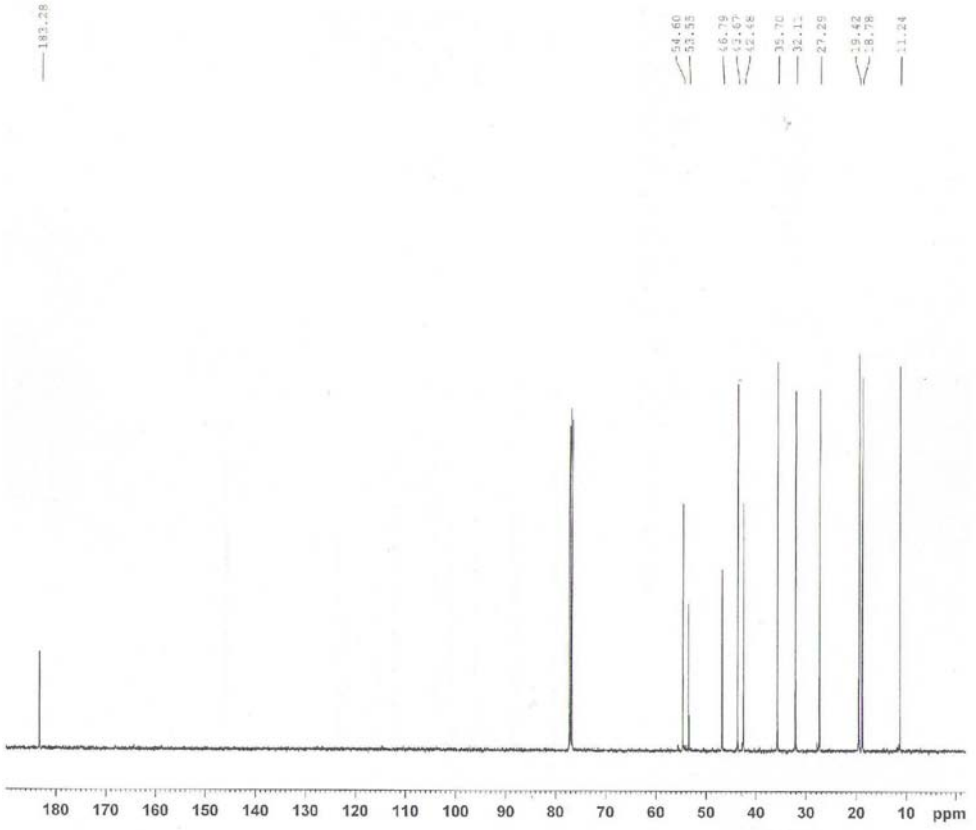

Figure S15. [13]C NMR spectrum of $\mathbf{2_B}$ ($CDCl_3$, 125 MHz).

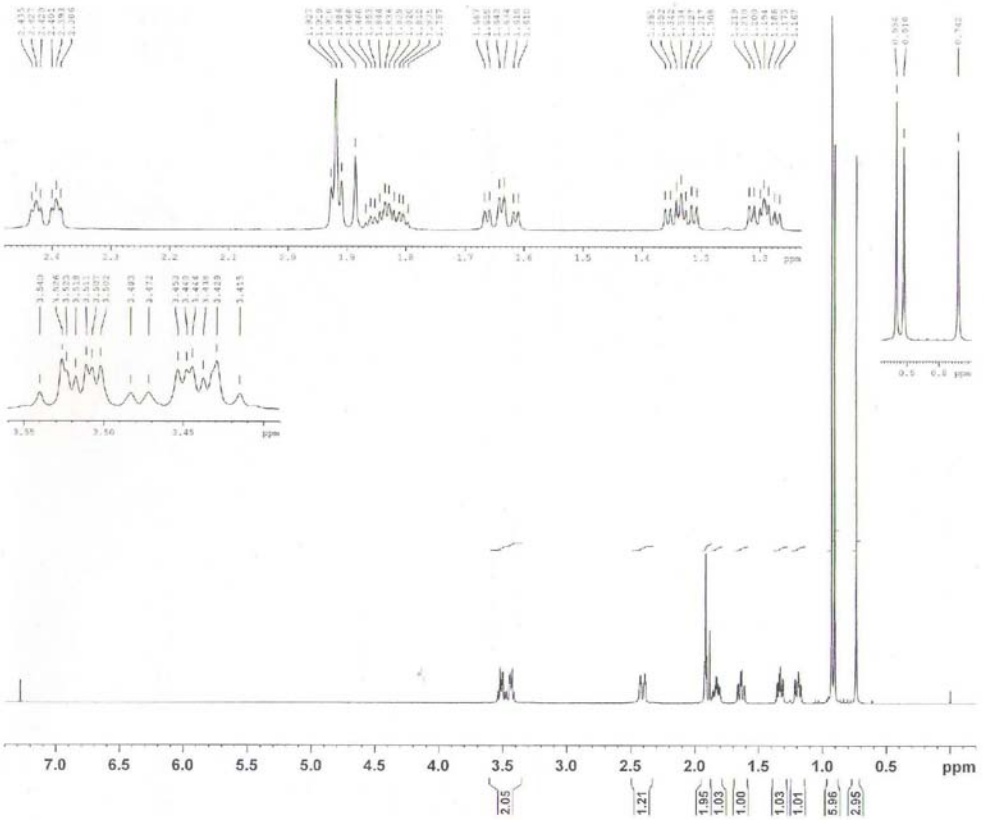

Figure S16. [1]H NMR spectrum of $\mathbf{2}_{\mathbf{C}}$ ($CDCl_3$, 500 MHz).

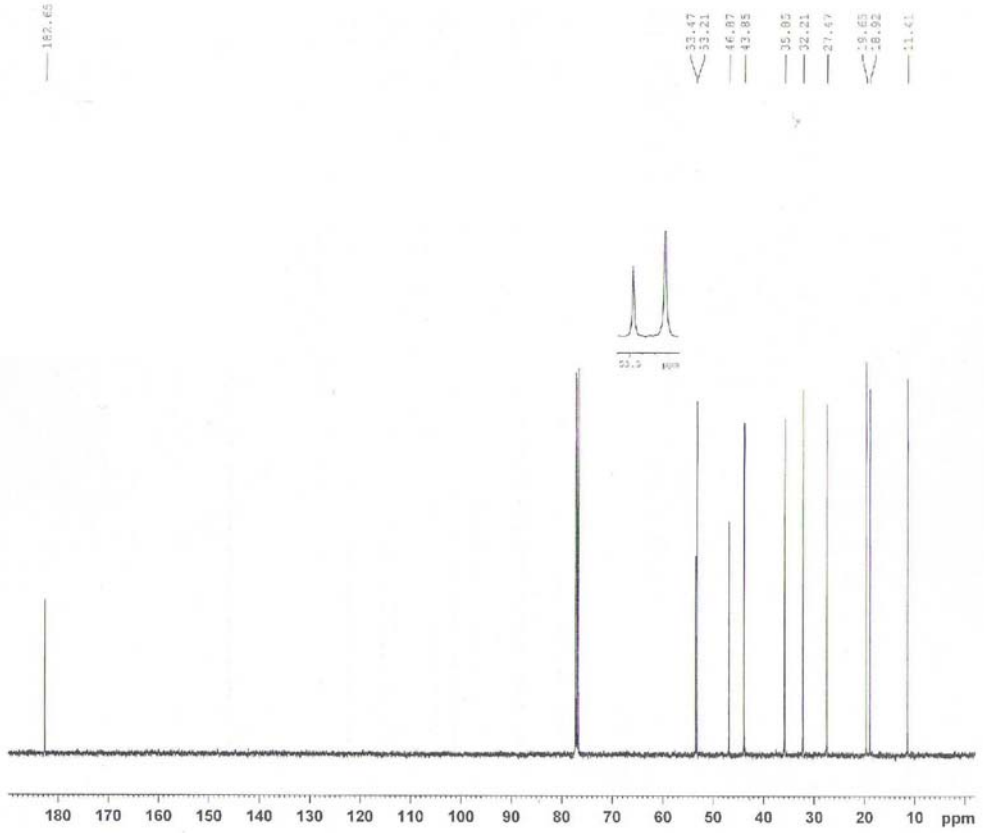

Figure S17. [13]C NMR spectrum of $\mathbf{2}_{\mathbf{C}}$ ($CDCl_3$, 125 MHz).

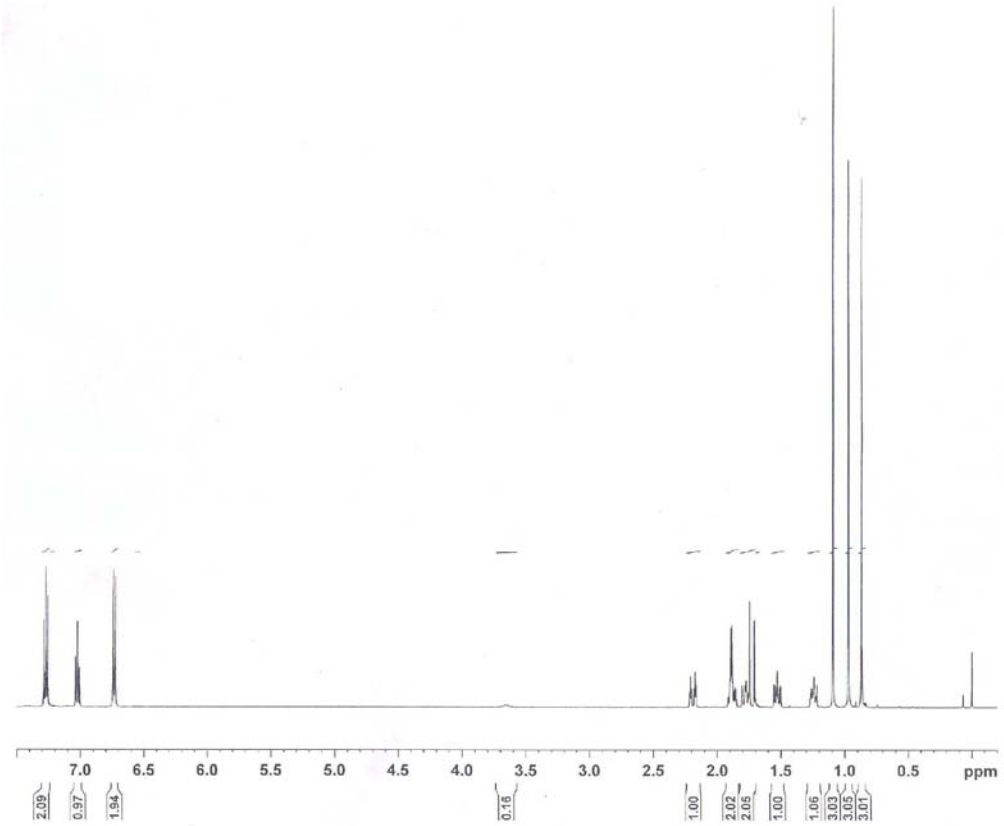

Figure S18. ^{1}H NMR spectrum of $\mathbf{2_D}$ ($CDCl_3$, 500 MHz).

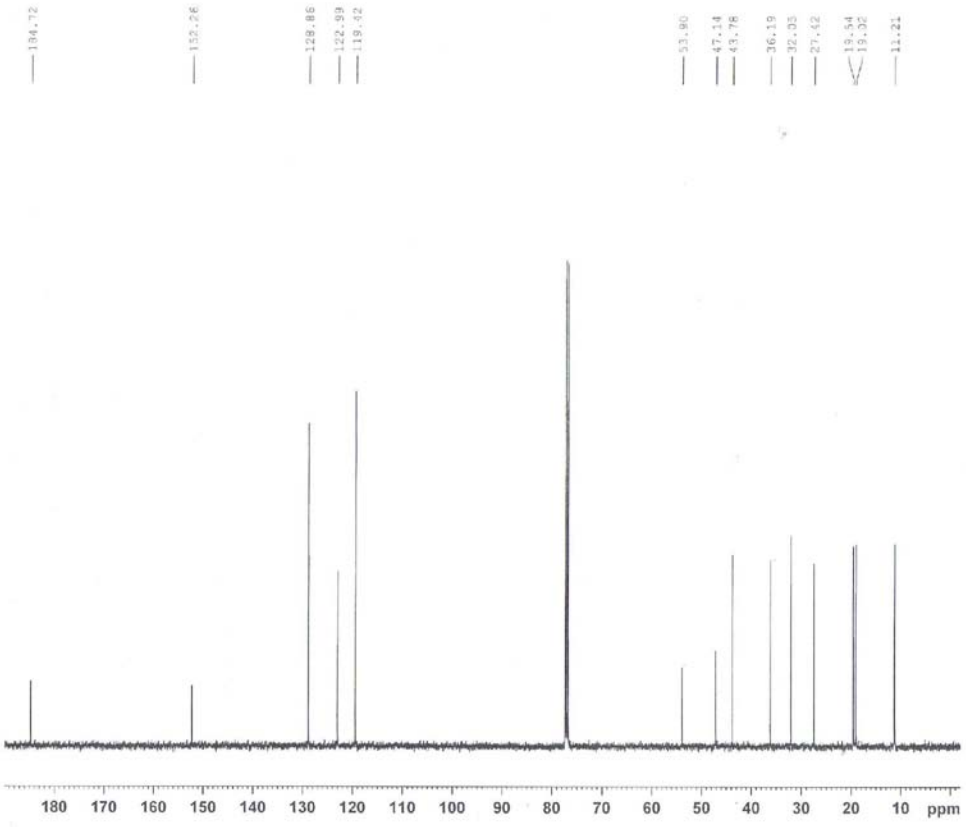

Figure S19. ^{13}C NMR spectrum of $\mathbf{2_D}$ ($CDCl_3$, 125 MHz).

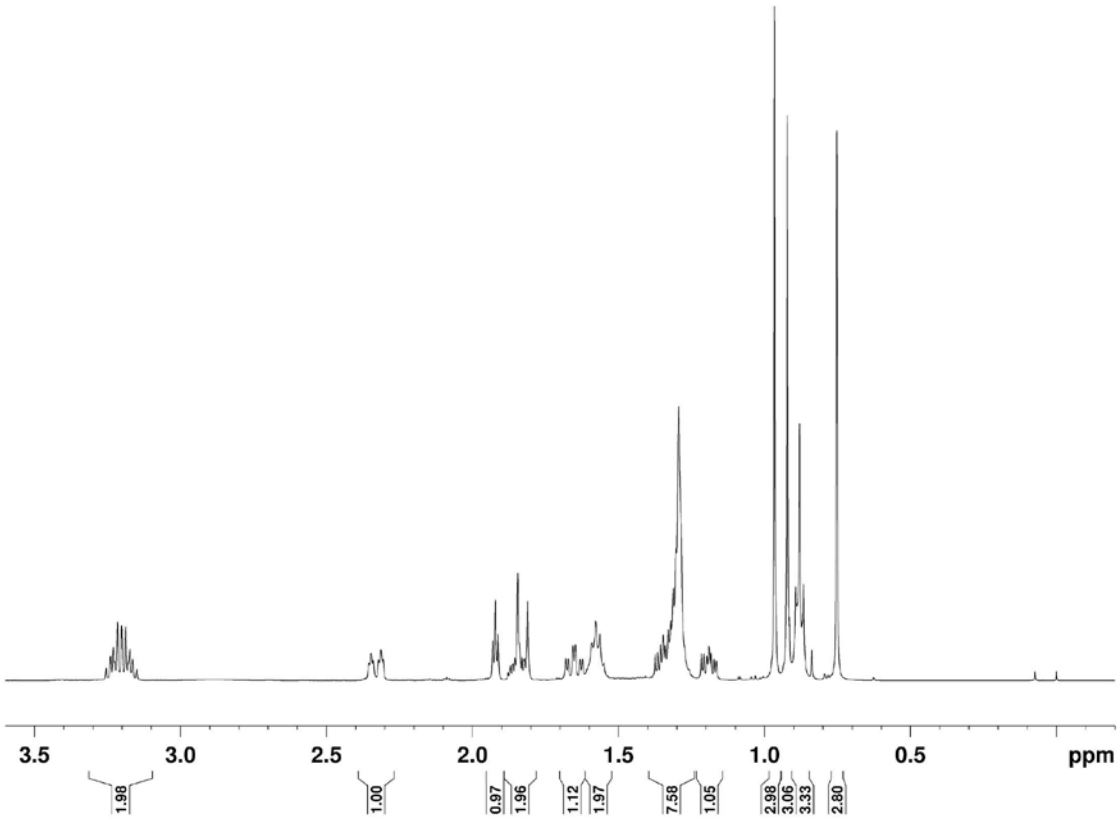

Figure S20. ^{1}H NMR spectrum of $\mathbf{2}_{E}$ ($CDCl_3$, 500 MHz).

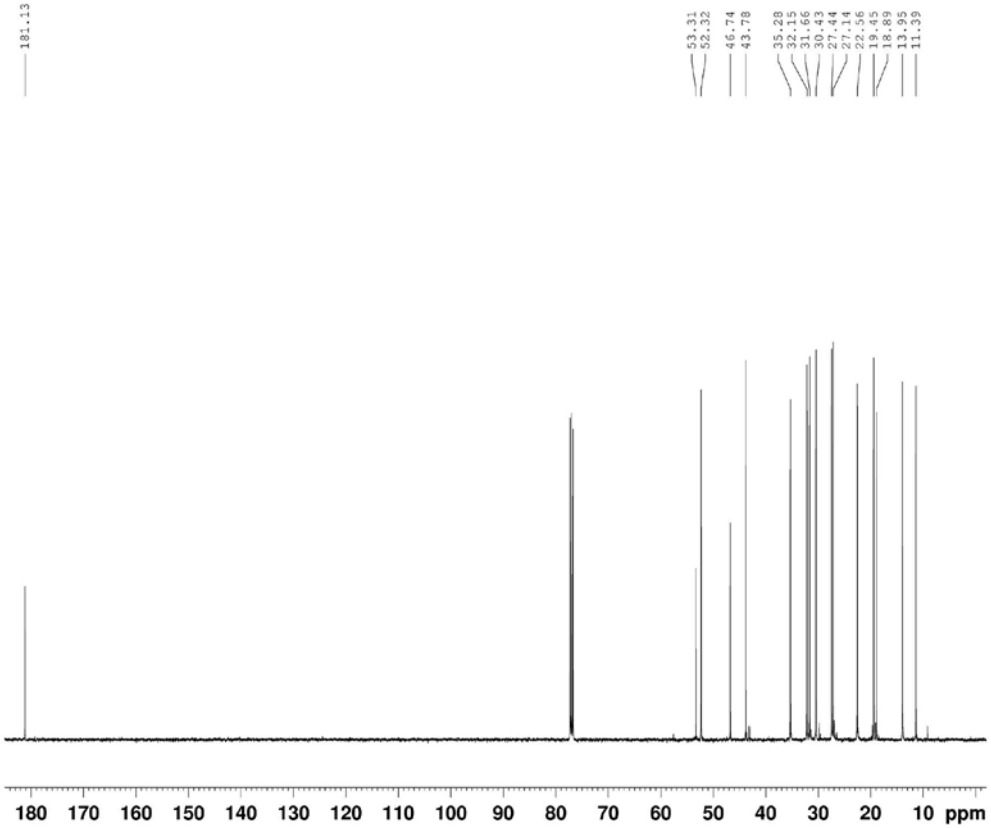

Figure S21. ^{13}C NMR spectrum of $\mathbf{2}_{E}$ ($CDCl_3$, 125 MHz).

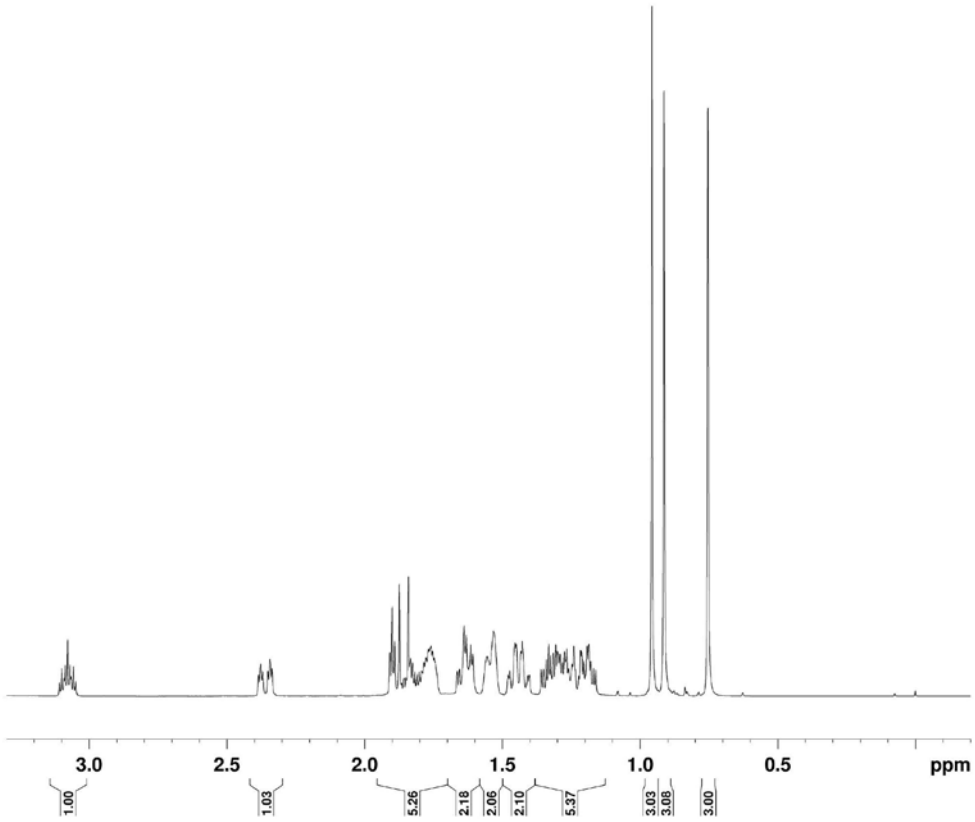

Figure S22. ^{1}H NMR spectrum of $\mathbf{2_F}$ ($CDCl_3$, 500 MHz).

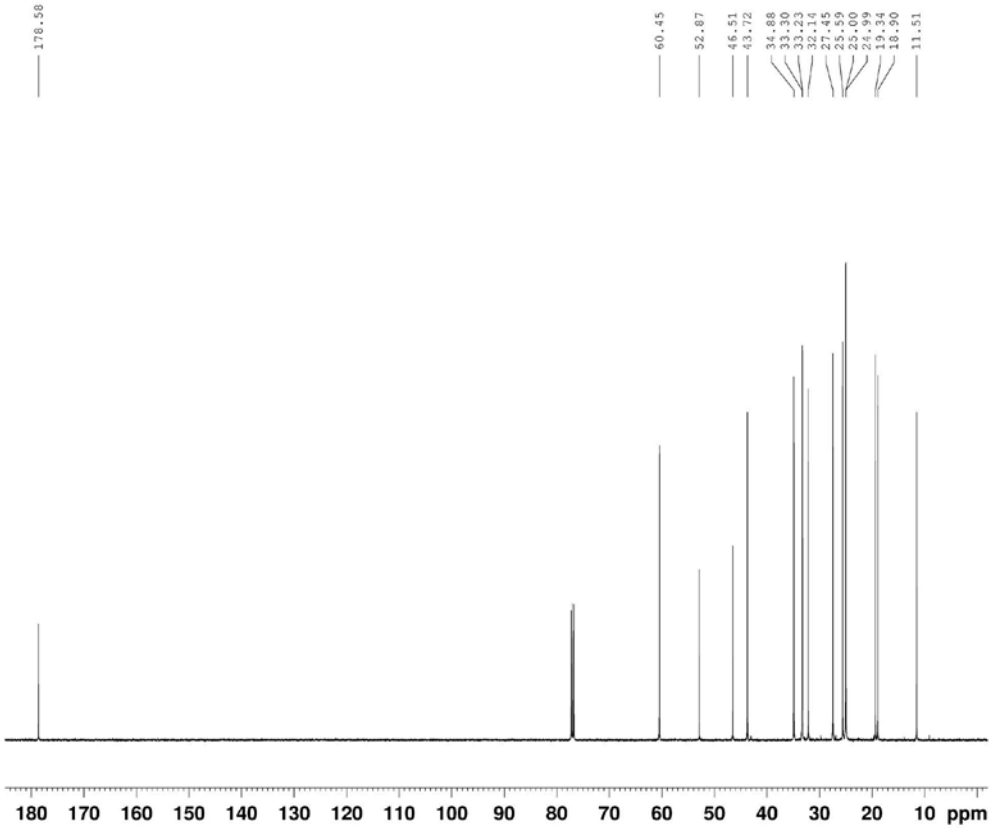

Figure S23. ^{13}C NMR spectrum of $\mathbf{2_F}$ ($CDCl_3$, 125 MHz).

Spectral data for $\mathbf{2}_{\mathbf{A-F}}$

2-(1,7,7-Trimethylbicyclo[2.2.1]heptan-2-ylidene) aminoethanol ($\mathbf{2}_{\mathbf{A}}$): a crude product was purified using chloroform/ethyl acetate 1:1 as an eluent to give $\mathbf{2}_{\mathbf{A}}$. White powder; yield: 0.771 g (73%); mp 65 °C; IR (KBr) ν/cm^{-1} 3418 ν(O–H), 2955, 2931 and 2870 ν(C–H), 1682 ν(C=N); ^{1}H NMR (500 MHz, $CDCl_3$) δ 0.75 (s, 3H, CH_3 (C9)), 0.93 (s, 3H, CH_3 (C8)), 0.97 (s, 3H, CH_3 (C10)), 1.21 (dtd, 1H, *J* 12.25, 9.00, 4.50 Hz, H_a5), 1.35 (dtd, 1H, *J* 13.00, 9.00, 4.50 Hz, H_a6), 1.67 (td, 1H, *J* 12.25, 4.50 Hz, H_e6), 1.84 (d, 1H, *J* 17.00 Hz, H_a3), 1.89 (m, 1H, H_e5), 1.95 (t, 1H, *J* 4.50 Hz, H4), 2.35 (dt, 1H, *J* 17.00, 3.50 Hz, H_e3), 3.31 (m, 2H, N–CH_2), 3.59 (br s, 1H, exchangeable with D_2O, OH), 3.79 (td, 2H, *J* 6.00, 0.50 Hz, CH_2–O); ^{13}C NMR (125 MHz, $CDCl_3$) δ 11.22 (C10), 18.81 (C8), 19.45 (C9), 27.28 (C5), 32.02 (C6), 35.94 (C3), 43.69 (C4), 47.05 (C7), 53.75 (C1 and C11, overlapped signals), 62.04 (C12), 184.53 (C=N). Anal. calcd. for $C_{12}H_{21}NO$ (195.31 g mol^{-1}): C, 73.80; H, 10.84; N, 7.17; found: C, 73.77; H, 10.85; N, 7.14.

N-(1,7,7-Trimethylbicyclo[2.2.1]heptan-2-ylidene) ethane-1,2-diamine ($\mathbf{2}_{\mathbf{B}}$): a crude product was purified by column chromatography on silica gel. First, ethyl acetate was applied to eluate $\mathbf{2}_{\mathbf{C}}$. Then, solvent was changed and $\mathbf{2}_{\mathbf{B}}$ was obtained using methanol as an eluent. White powder; yield: 0.641 g (61%); mp 49 °C; IR (KBr) ν/cm^{-1} 3435 ν(N–H), 2956, 2921 and 2873 ν(C–H), 1686 ν(C=N); ^{1}H NMR (500 MHz, $CDCl_3$) δ 0.75 (s, 3H, CH_3 (C9)), 0.93 (s, 3H, CH_3 (C8)), 0.97 (s, 3H, CH_3 (C10)), 1.20 (dtd, 1H, *J* 12.25, 9.00, 4.50 Hz, H_a5); 1.34, (dtd, 1H, *J* 13.00, 9.00, 4.50 Hz, H_a6), 1.67 (td, 1H, *J* 12.25, 4.50 Hz, H_e6), 1.85 (d, 1H, *J* 17.00 Hz, H_a3), 1.86 (m, 1H, H_e5), 1.94 (t, 1H, *J* 4.50 Hz, H4), 1.98 (br s, 2H, exchangeable with D_2O, NH_2), 2.35 (dt, 1H, *J* 17.00, 3.50 Hz, H_e3), 2.93 (m, 2H, CH_2–N), 3.25 (m, 2H, N–CH_2); ^{13}C NMR (125 MHz, $CDCl_3$) δ 11.24 (C10), 18.78 (C8), 19.42 (C9), 27.29 (C5), 32.11 (C6), 35.70 (C3), 42.48 (C12), 43.67 (C4), 46.79 (C7), 53.55 (C1), 54.60 (C11), 184.53 (C=N). Anal. calcd. for $C_{12}H_{22}N_2$ (194.32 g mol^{-1}): C, 74.17; H, 11.41; N, 14.42; found: C, 74.97; H, 11.71; N, 14.76.

N^1-(1,7,7-Trimethylbicyclo[2.2.1]heptan-2-ylidene)-*N*^{2}-(1,7,7-trimethylbicyclo [2.2.1]heptan-2-ylidene)ethane-1,2-diamine ($\mathbf{2}_{\mathbf{C}}$): a crude product was purified using ethyl acetate as an eluent to give $\mathbf{2}_{\mathbf{C}}$. White powder; yield: 0.261 g (29%); mp 51 °C; IR (KBr) ν/cm^{-1} 2956, 2921 and 2872 ν(C–H), 1686 ν(C=N); ^{1}H NMR (500 MHz, $CDCl_3$) δ 0.74 (s, 3H, CH_3 (C9)), 0.91 (s, 3H, CH_3 (C8)), 0.93 (s, 3H, CH_3 (C10)), 1.19 (dtd, 1H, *J* 12.25, 9.00, 4.50 Hz, H_a5), 1.33 (dtd, 1H, *J* 13.00, 9.00, 4.50 Hz, H_a6), 1.64 (td, 1H, *J* 12.25, 4.50 Hz, H_e6), 1.87 (m, 1H, H_e5), 1.90 (d, 1H, *J* 17.00 Hz, H_a3), 1.92 (t, 1H, *J* 4.50 Hz, H4), 2.41 (dt, 1H, *J* 17.00, 3.50 Hz, H_e3), 3.44, (m, 1H, N–CH_2), 3.51 (m, 1H, N–CH_2); ^{13}C NMR (125 MHz, $CDCl_3$) δ 11.41 (C10), 18.92 (C8), 19.65 (C9), 27.47 (C5), 32.21 (C6), 35.85 (C3), 43.85 (C4), 46.87 (C7), 53.21 (C11), 53.47 (C1), 184.53 (C=N). Anal. calcd. for $C_{22}H_{36}N_2$ (328.54 g mol^{-1}): C, 80.43; H, 11.05; N, 8.53; found: C, 80.74; H, 11.18; N, 8.86.

N-(1,7,7-Trimethylbicyclo[2.2.1]heptan-2-ylidene)aniline ($\mathbf{2}_{\mathbf{D}}$): a crude product was purified using chloroform as an eluent to give $\mathbf{2}_{\mathbf{D}}$. Yellowish oil; yield: 0.195 g (16%); IR (neat) ν/cm^{-1} 3079 $\nu(C–H)_{Ar}$, 2958, and 2873 ν(C–H), 1685 ν(C=N); ^{1}H NMR (500 MHz, $CDCl_3$) δ 0.87 (s, 3H, CH_3 (C9)), 0.97 (s, 3H, CH_3 (C8)), 1.09 (s, 3H, CH_3 (C10)), 1.24 (m, 1H, H_a5), 1.53 (dtd, 1H, *J* 12.50, 9.50, 4.00 Hz, H_a6), 1.73 (d, 1H, *J* 18.00 Hz, H_a3), 1.78 (m, 1H, H_e6), 1.88 (m, 1H, H_e5), 1.89 (d, 1H, *J* 4.00 Hz, H4), 2.19 (dt, 1H, *J* 18.00, 4.00 Hz, H_e3), 6.73 (dd, 2H, *J* 7.50, 1.00 Hz, *o*-phenyl), 7.02 (tt, 1H, *J* 7.50, 1.00 Hz, p-phenyl), 7.27 (td, 2H, *J* 7.50, 1.00 Hz, m-phenyl); ^{13}C NMR (125 MHz, $CDCl_3$) δ 11.21 (C10), 19.02 (C8), 19.54 (C9), 27.42 (C5), 32.05 (C6), 36.19 (C3), 43.78 (C4), 47.14 (C7), 53.90 (C1), 119.42 (C12), 122.99 (C14), 128.86 (C13), 152.26 (C11), 184.72 (C=N). Anal. calcd. for $C_{16}H_{21}N$ (227.35 g mol^{-1}): C, 84.53; H, 9.31; N, 6.16; found: C, 84.74; H, 9.52; N, 6.41.

N-(1,7,7-Trimethylbicyclo[2.2.1]heptan-2-ylidene) hexan-1-amine ($\mathbf{2}_{\mathbf{E}}$): a crude product was purified using chloroform/ethyl acetate, 9.5:0.5 as an eluent to give $\mathbf{2}_{\mathbf{E}}$. Yellowish oil; yield: 0.327 g (26%); IR (neat) ν/cm^{-1} 2954, 2927, 2872 and 2857 ν(C–H), 1686 ν(C=N); ^{1}H NMR (500 MHz, $CDCl_3$) δ 0.75 (s, 3H, CH_3 (C9)), 0.87 (t, 3H, *J* 6.50 Hz, CH_3 (C16)), 0.92 (s, 3H, CH_3 (C8)), 0.97 (s, 3H, CH_3 (C10)), 1.19 (dtd, 1H, *J* 12.25, 9.00, 4.50 Hz, H_a5), 1.29 (m, 6H, (C13, C14, C15)), 1.36 (dtd, 1H, *J* 13.00, 9.00, 4.50 Hz, H_a6), 1.58 (m, 2H, (C12)), 1.65 (td, 1H, *J* 12.25, 4.50 Hz, H_e6), 1.83 (d, 1H, *J* 17.00 Hz, H_a3), 1.85 (m, 1H, H_e5), 1.92 (t, 1H, *J* 4.50 Hz, H4), 2.33 (dt, 1H, *J* 17.00, 3.50 Hz, H_e3), 3.20 (m, 2H, CH_2 (C11)); ^{13}C NMR (125 MHz, $CDCl_3$) δ 11.39 (C10), 13.95 (C16), 18.89 (C8), 19.45 (C9), 22.56 (C15), 27.14 (C13), 27.44 (C5), 30.43 (C12), 31.66 (C14), 32.15 (C6), 35.28 (C3), 43.78 (C4), 46.74 (C7), 52.32 (C11), 53.31 (C1), 181.13 (C=N). Anal. calcd. for $C_{16}H_{29}N$ (235.41 g mol^{-1}): C, 81.63; H, 12.42; N, 5.95; found: C, 81.94; H, 12.58; N, 6.13.

N-(1,7,7-Trimethylbicyclo[2.2.1]heptan-2-ylidene) cyclohexanamine ($\mathbf{2}_{\mathbf{F}}$): a crude product was purified using chloroform as an eluent to give $\mathbf{2}_{\mathbf{F}}$. Yellowish oil; yield:

0.175 g (14%); IR (neat) ν/cm^{-1} 2925 and 2853 ν(C–H), 1685 ν(C=N); ^{1}H NMR (500 MHz, $CDCl_3$) δ 0.75 (s, 3H, CH_3 (C9)), 0.91 (s, 3H, CH_3 (C8)), 0.96 (s, 3H, CH_3 (C10)), 1.16-1.36 (m, 5H, H_a5, 3H (Cy), H_a6), 1.44 (m, 2H, Cy), 1.54 (m, 2H, Cy), 1.64 (m, 2H, 1H, Cy, H_e6), 1.76 (m, 2H, Cy), 1.83 (m, 1H, H_e5), 1.86 (d, 1H, *J* 17.00 Hz, H_a3), 1.90 (t, 1H, *J* 4.50 Hz, H4), 2.36 (dt, 1H, *J* 17.00, 4.00 Hz, H_e3), 3.08 (m, 1H, CH (C11)); ^{13}C NMR (125 MHz, $CDCl_3$) δ 11.51 (C10), 18.90 (C8), 19.34 (C9), 24.99 and 25.00 (C13 and C13'), 25.59 (C14), 27.45 (C5), 32.14 (C6), 33.23 and 33.30 (C12 and C12'), 34.88 (C3), 43.72 (C4), 46.51 (C7), 52.87 (C1), 60.45 (C11), 178.58 (C=N). Anal. calcd. for $C_{16}H_{27}N$ (233.40 g mol^{-1}): C, 82.34; H, 11.66; N, 6.00; found: C, 82.67; H, 11.71; N, 6.11.

Experimental and calculated geometrical parameters of $\mathbf{2_A}$

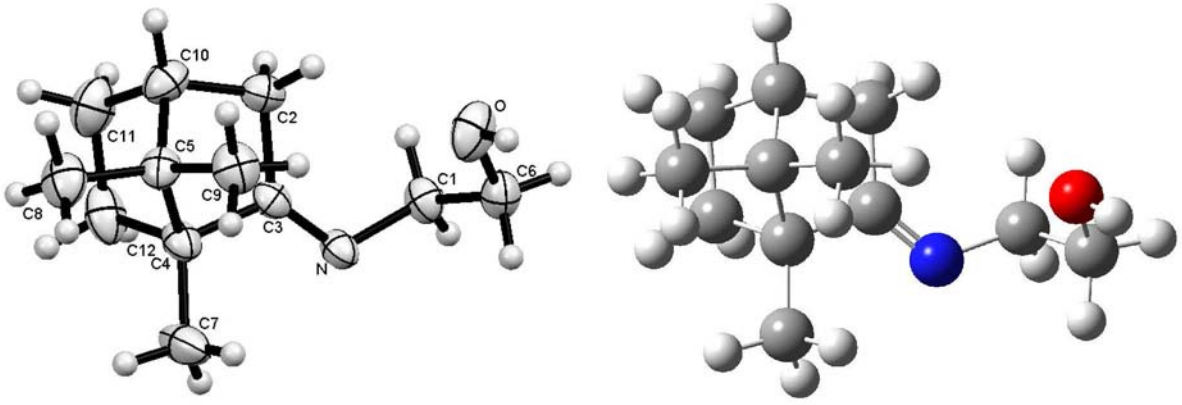

Figure S24. Crystal structure (left) and calculated structure of $\mathbf{2_A}$ in the gas-phase.

Table S1. Experimental and calculated bond distances between heavy atoms in $\mathbf{2_A}$. See Figure S1 for atom labeling

Bond distance / Å	Experimental	Calculated
C1–C6	1.5135	1.5222
C1–N	1.4710	1.4556
C2–C3	1.5190	1.5356
C2–C10	1.5289	1.5437
C3–C4	1.5188	1.5288
C3–N	1.2693	1.2666
C4–C5	1.5688	1.5758
C4–C7	1.5211	1.5175
C4–C12	1.5495	1.5633
C5–C8	1.5343	1.5366
C5–C9	1.5292	1.5389
C5–C10	1.5454	1.5619
C6–O	1.4090	1.4324
C10–C11	1.5452	1.5466
C11–C12	1.5334	1.5590

Table S2. Experimental and calculated bond angles between heavy atoms in $\mathbf{2_A}$. See Figure S1 for atom labeling

Bond angle / degree	Experimental	Calculated
C1–C6–O	109.8	108.4
C1–N–C3	118.4	119.9
C2–C3–N	129.8	130.4
C2–C10–C5	102.7	102.6
C2–C10–C11	106.1	106.8
C3–C2–C10	102.4	101.8
C3–C4–C5	100.4	100.5
C3–C4–C7	115.8	115.0
C3–C4–C12	104.2	104.2
C4–C5–C8	114.3	114.5
C4–C5–C9	113.1	113.5
C4–C5–C10	93.5	93.4
C4–C12–C11	104.6	104.2
C5–C4–C7	117.1	118.6
C5–C4–C12	101.7	101.8
C5–C10-C11	102.7	102.9
C6–C1–N	111.9	110.8
C7–C4–C12	115.4	114.5
C8–C5–C9	108.2	107.6
C8–C5–C10	113.6	113.7
C9–C5–C10	113.8	113.9
C10–C11–C12	102.8	102.8

Table S3. Experimental and calculated values for selected dihedral angles in $\mathbf{2}_{A}$. See Figure S1 for atom labeling

Dihedral angle / degree	Experimental	Calculated	Dihedral angle / degree	Experimental	Calculated
C1–N–C3–C4	179.0	179.4	C5–C4–C3–N	145.0	144.9
C2–C3–C4–C5	35.0	34.5	C7–C4–C5–C8	62.2	62.1
C2–C3–C4–C7	162.1	163.2	C7–C4–C5–C9	62.2	62.0
C2–C3–C4–C12	70.0	70.6	C7–C4–C5–C10	180.0	180.0
C2–C10–C11–C12	70.6	71.1	C7–C4–C12–C11	160.9	162.7
C3–C2–C10–C5	35.1	35.7	C8–C5–C10–C2	173.3	174.0
C3–C2–C10–C11	72.4	72.2	C8–C5–C10–C11	63.2	63.2
C3–C4–C5–C8	171.6	171.7	C9–C5–C10–C2	62.3	62.4
C3–C4–C5–C9	64.0	64.3	C9–C5–C10–C11	172.4	173.1
C3–C4–C5–C10	53.8	53.6	C10–C2–C3–N	179.5	179.7
C3–C4–C12–C11	71.0	70.8	C12–C4–C5–C9	171.0	171.4
C4–C5–C10–C2	54.8	55.3	C12–C4–C5–C8	64.6	64.6
C4–C5–C10–C11	55.2	55.5	C12–C4–C5–C10	53.2	53.4
C5–C4–C12–C11	33.0	33.4	C12–C4–C3–N	110.0	109.9
C5–C10–C11–C12	36.8	36.6	N–C1–C6–O	70.3	71.8

Results of DFT calculations

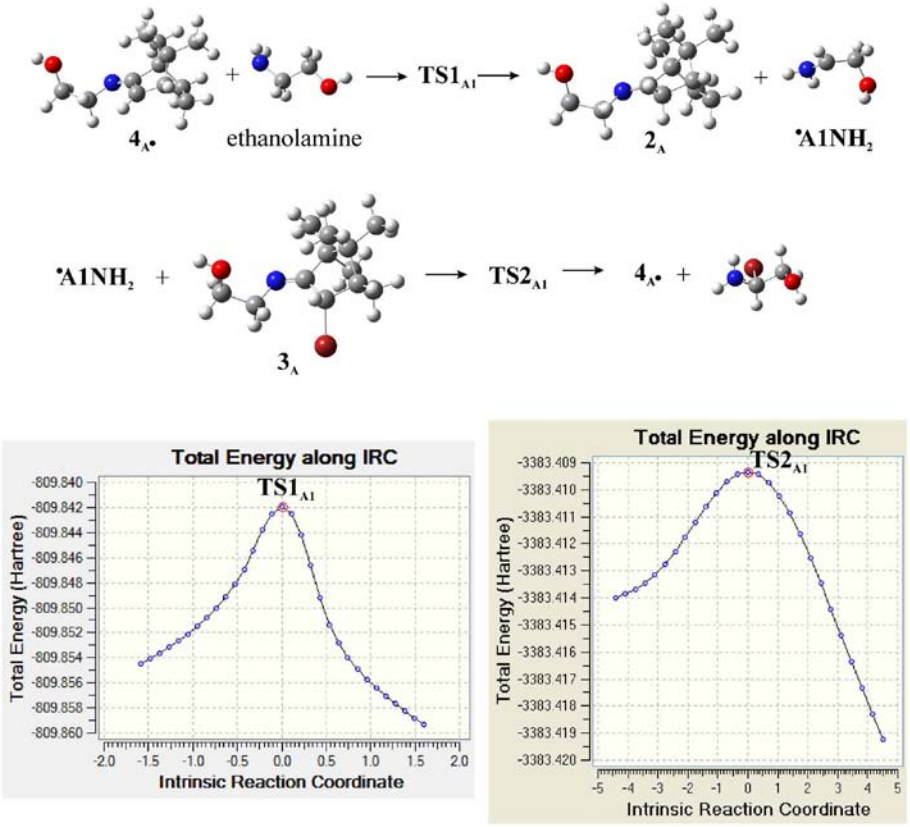

Figure S25. Optimized geometries of the reactants and products in the elementary steps 13 and 14, where ethanolamine reacts in the position 11. Results of the IRC calculations for the corresponding transition states.

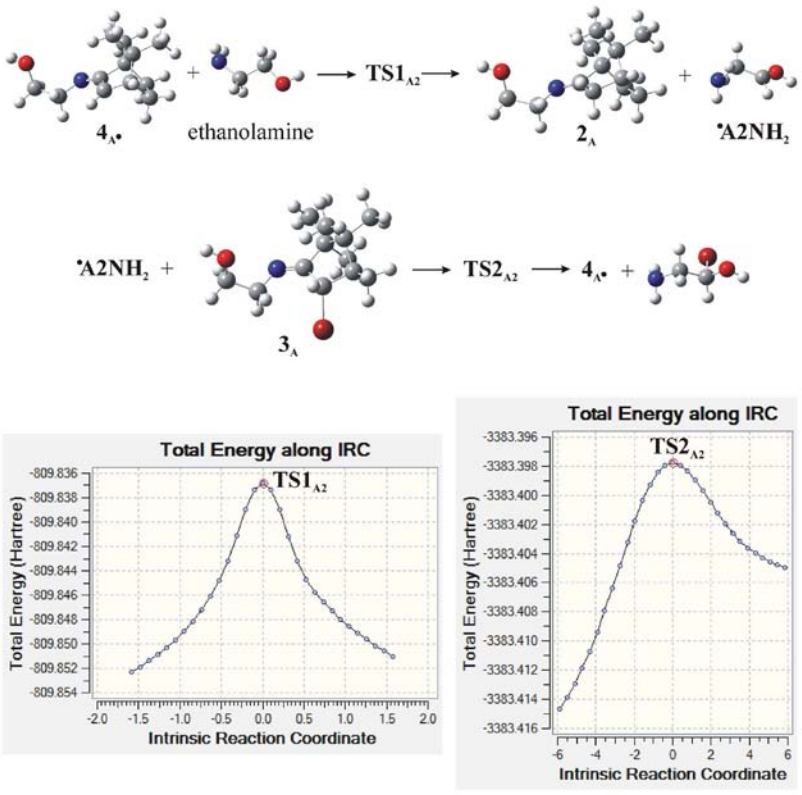

Figure S26. Optimized geometries of the reactants and products in the elementary steps 13 and 14, where ethanolamine reacts in the position 12. Results of the IRC calculations for the corresponding transition states.

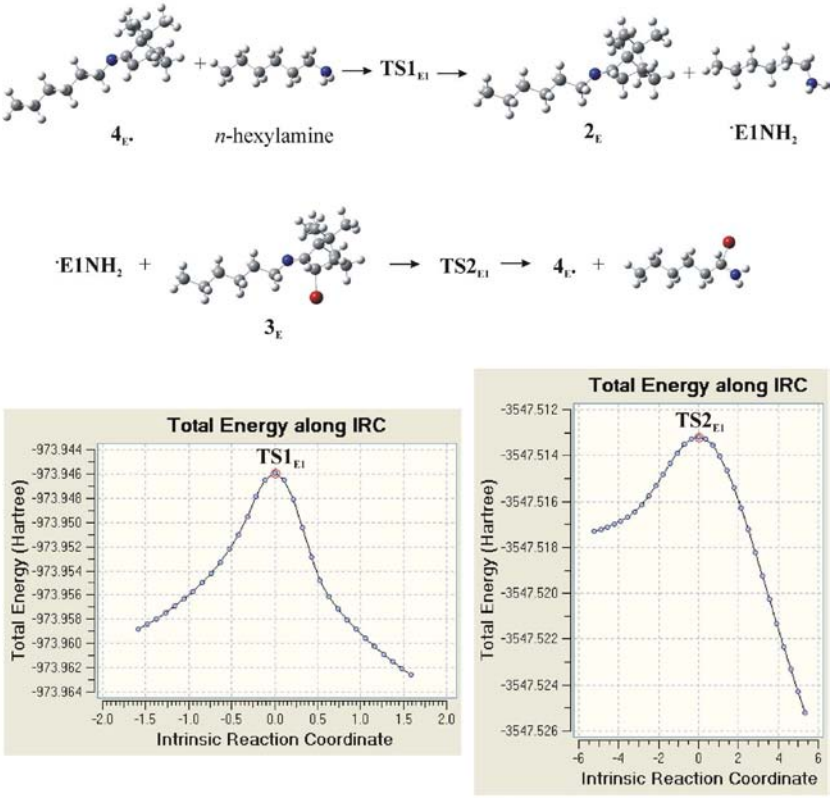

Figure S27. Optimized geometries of the reactants and products in the elementary steps 13 and 14, where *n*-hexylamine reacts in the position 11. Results of the IRC calculations for the corresponding transition states.

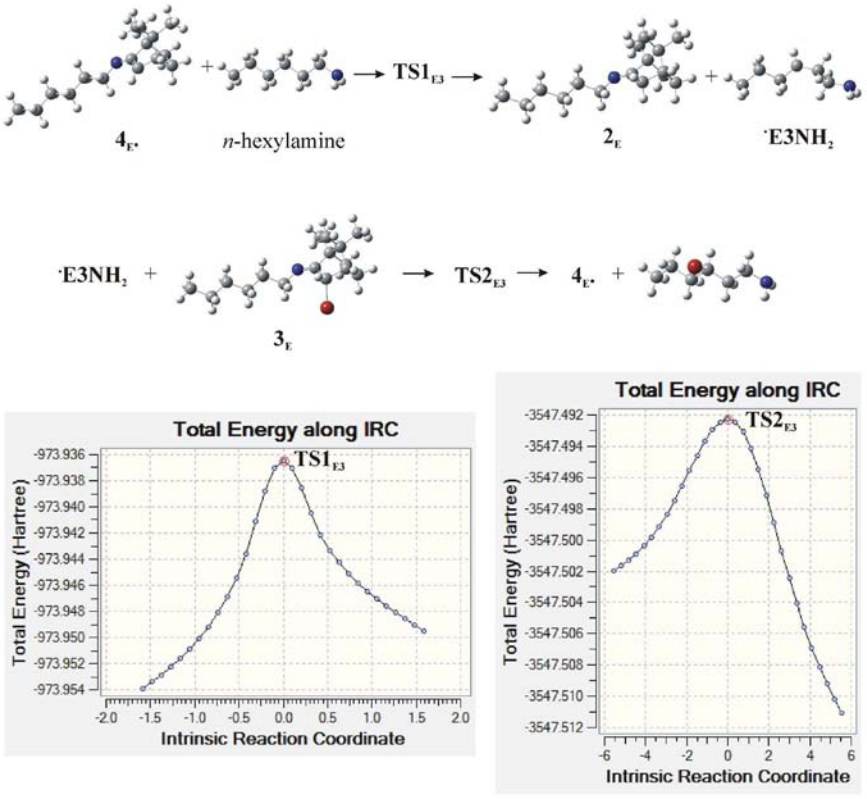

Figure S28. Optimized geometries of the reactants and products in the elementary steps 13 and 14, where *n*-hexylamine reacts in the position 13. Results of the IRC calculations for the corresponding transition states.